

NEWS AND VIEWS

Systems biology flowering in the plant clock field

Hiroki R Ueda

Center for Developmental Biology, RIKEN, Chuo-ku, Kobe, Hyogo, Japan

Molecular Systems Biology 14 November 2006; doi:10.1038/msb4100105

In the 18th Century, the Swedish botanist Karl von Linné designed a 'Flower-Clock' by arranging a series of various plant species according to the respective time their flowers open or close every day. Watching this 'Flower-Clock', one can then estimate the time of the day by noting the pattern of flower opening and closing. It has been a well-known fact since Linné's early times that plants can open or close their flowers at a precise time of the day. However, we still do not fully understand the design principles of the molecular network that underlies the cellular circadian clock, which achieves to predict, often with exquisite precision, the cyclic changes in the environment due to the rotation of earth. In two articles currently published in *Molecular Systems Biology*, Millar and co-workers (Locke *et al.*, 2006) and Doyle and co-workers (Zeilinger *et al.*, 2006) propose a plausible design for the plant circadian clock.

In previous work, Millar and co-workers extended an initial 'one-loop model' of the plant circadian clock into a 'two-loop model' (Figure 1) (Locke *et al.*, 2005). In the simple 'one-loop model' (Figure 1, loop I), two partially redundant genes, LATE ELONGATED HYPOCOTYL (LHY) and CIRCADIAN CLOCK ASSOCIATED 1 (CCA1), repress the expression of their activator, TIMING OF CAB EXPRESSION 1 (TOC1) (Alabadi *et al.*, 2001). In this model, light activates the expression of LHY/CCA1, according to experimental data that show a response of LHY and CCA1 transcription to light stimulation (Wang and Tobin, 1998; Martinez-Garcia *et al.*, 2000; Kim *et al.*, 2003). The simple 'one-loop model' cannot explain some experimental data, such as the short period rhythm in *lhy;cca1* mutants (Alabadi *et al.*, 2002; Locke *et al.*, 2005). In order to explain the residual rhythm in *lhy;cca1* plants, Millar and co-workers incorporated two hypothetical components, X and Y, to develop a 'two-loop model' (Figure 1, loops I and II). In this extended model, TOC1 is proposed to activate the expression of X, which, in turn, activates LHY/CCA1 transcription, as required by the time-course profile of TOC1 protein (Mas *et al.*, 2003b). The second loop is formed by Y and TOC1, and is responsible for the short-period oscillation in the *lhy;cca1* mutant. Y is also proposed to be activated by light, because TOC1 transcription has been shown to respond to light, although there is no evidence of direct light activation of TOC1 transcription (Makino *et al.*, 2001). Although the 'two-loop model' can explain many aspects of plant circadian clocks (Locke *et al.*, 2005), it still cannot explain some experimental data, including the residual short-period rhythm observed in the *toc1* mutants (Mas *et al.*, 2003a) and the very long-period rhythm of double mutants for PSEUDO-RESPONSE REGULATOR 7 (PRR7) and PRR9 (Farre *et al.*, 2005).

In order to explain the latter experimental results, Millar and co-workers (Locke *et al.*, 2006) and Doyle and co-workers (Zeilinger *et al.*, 2006) incorporated the recently proposed feedback loop between PRR7/PRR9 and LHY/CCA1 (Farre *et al.*, 2005; Salome and McClung, 2005) and proposed a further extension of the model into a 'three-loop model' (Figure 1, loops I–III). In this new model, PRR7/PRR9 are proposed to be activated by LHY/CCA1, although PRR7/PRR9 proteins repress LHY/CCA1 transcription. Light activates the expression of PRR7/PRR9 in Millar's study, or PRR9 in Doyle's model, as PRR9 has been shown to be acutely activated by light (Ito *et al.*, 2003). Millar's and Doyle's models are very similar in their global structure, but differ slightly in how light induction of Y and LHY/CCA1 is modeled, and in the details of the PRR7/PRR9-LHY/CCA1 loop mechanism. For example, Millar's model assumes that light induction of Y and LHY/CCA1 depends on both a continuous and a transient mechanism, whereas Doyle and co-workers propose a more sophisticated mechanism, whereby light induction of Y is dependent on a continuous mechanism, whereas that of LHY/CCA1 is dependent on a transient mechanism. For the purpose of simplification, PRR7/PRR9 are dealt as one factor in Millar's work, whereas PRR7 and PRR9 are more realistically treated as two different factors in Doyle's model. It is also noteworthy that Millar and co-workers analyzed the rhythms of *gi;lhy;cca1* triple mutant plants to further experimentally validate

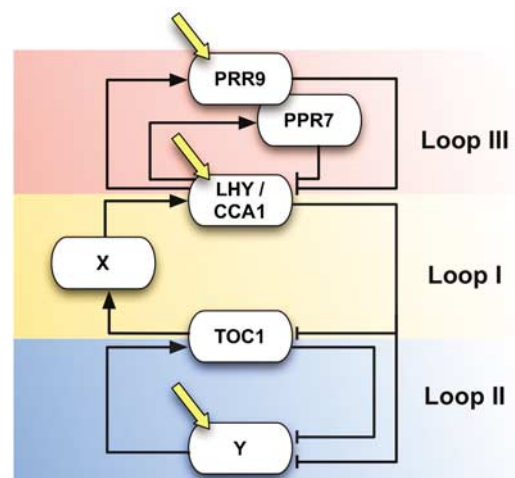


Figure 1 Schematic representation of the proposed models of the plant circadian clock. X and Y are hypothetical proteins. Yellow arrows indicate light input.

their proposal that GI is a strong candidate for being part of the hypothetical Y component (Locke *et al.*, 2006), and that Doyle's and co-workers performed a detailed sensitivity analysis to identify the points of strength and weakness in the current 'three-loop model', thus providing a guide for future experimental and modeling efforts (Zeilinger *et al.*, 2006).

In both cases, the 'three-loop model' suggests an interesting design principle underlying the plant clock. The morning oscillator, PRR7/PRR9-LHY/CCA1 loop (Figure 1, loop III), and the evening oscillator, TOC1-Y loop (Figure 1, loop II), are coupled together via the LHY/CCA1-TOC1-X loop (Figure 1, loop I). These coupled morning and evening oscillators may provide the flexibility to track dawn and dusk and, thus, confer the clock with the capability of measuring the length of the day (or intervals of multiple phases) under conditions of changing photoperiods. In order to formally prove the proposed 'three-loop model', it will be necessary to uncover the identity of the missing factor X linking the morning and evening oscillators. Only time will tell how plausible biologically significant the 'three-loop model' really is, but the perspective that an X mutation will cause the morning and evening oscillators to run with different periods within the same cell is surely an exciting one. We can only hope that such a discovery will be reported in the near future!

References

- Alabadi D, Oyama T, Yanovsky MJ, Harmon FG, Mas P, Kay SA (2001) Reciprocal regulation between TOC1 and LHY/CCA1 within the *Arabidopsis* circadian clock. *Science* **293**: 880–883
- Alabadi D, Yanovsky MJ, Mas P, Harmer SL, Kay SA (2002) Critical role for CCA1 and LHY in maintaining circadian rhythmicity in *Arabidopsis*. *Curr Biol* **12**: 757–761
- Farre EM, Harmer SL, Harmon FG, Yanovsky MJ, Kay SA (2005) Overlapping and distinct roles of PRR7 and PRR9 in the *Arabidopsis* circadian clock. *Curr Biol* **15**: 47–54
- Ito S, Matsushika A, Yamada H, Sato S, Kato T, Tabata S, Yamashino T, Mizuno T (2003) Characterization of the APRR9 pseudo-response regulator belonging to the APRR1/TOC1 quintet in *Arabidopsis thaliana*. *Plant Cell Physiol* **44**: 1237–1245
- Kim JY, Song HR, Taylor BL, Carre IA (2003) Light-regulated translation mediates gated induction of the *Arabidopsis* clock protein LHY. *EMBO J* **22**: 935–944
- Locke JCW, Kozma-Bognar L, Gould PD, Fehér B, Kevei É, Nagy F, Turner MS, Hall A, Millar AJ (2006) Experimental validation of a predicted feedback loop in the multi-oscillator clock of *Arabidopsis thaliana*. *Mol Syst Biol* **2**: 59
- Locke JCW, Southern MM, Kozma-Bognar L, Hibberd V, Brown PE, Turner MS, Millar AJ (2005) Extension of a genetic network model by iterative experimentation and mathematical analysis. *Mol Syst Biol* **1**: 13
- Makino S, Matsushika A, Kojima M, Oda Y, Mizuno T (2001) Light response of the circadian waves of the APRR1/TOC1 quintet: when does the quintet start singing rhythmically in *Arabidopsis*? *Plant Cell Physiol* **42**: 334–339
- Martinez-Garcia JF, Huq E, Quail PH (2000) Direct targeting of light signals to a promoter element-bound transcription factor. *Science* **288**: 859–863
- Mas P, Alabadi D, Yanovsky MJ, Oyama T, Kay SA (2003a) Dual role of TOC1 in the control of circadian and photomorphogenic responses in *Arabidopsis*. *Plant Cell* **15**: 223–236
- Mas P, Kim WY, Somers DE, Kay SA (2003b) Targeted degradation of TOC1 by ZTL modulates circadian function in *Arabidopsis thaliana*. *Nature* **426**: 567–570
- Salome PA, McClung CR (2005) Pseudo-response regulator 7 and 9 are partially redundant genes essential for the temperature responsiveness of the *Arabidopsis* circadian clock. *Plant Cell* **17**: 791–803
- Wang ZY, Tobin EM (1998) Constitutive expression of the circadian clock associated 1 (CCA1) gene disrupts circadian rhythms and suppresses its own expression. *Cell* **93**: 1207–1217
- Zeilinger MN, Farré EM, Taylor SR, Kay SA, Doyle III FJ (2006) A novel computational model of the circadian clock in *Arabidopsis* that incorporates PRR7 and PRR9. *Mol Syst Biol* **2**: 58

REPORT

Experimental validation of a predicted feedback loop in the multi-oscillator clock of *Arabidopsis thaliana*

James CW Locke^{1,2,3,7}, László Kozma-Bognár⁴, Peter D Gould⁵, Balázs Fehér⁶, Éva Kevei⁶, Ferenc Nagy⁶, Matthew S Turner^{2,3}, Anthony Hall^{5,*} and Andrew J Millar^{3,4,*}

¹ Department of Biological Sciences, University of Warwick, Coventry, UK, ² Department of Physics, University of Warwick, Coventry, UK, ³ Interdisciplinary Programme for Cellular Regulation, University of Warwick, Coventry, UK, ⁴ Institute of Molecular Plant Sciences, University of Edinburgh, Edinburgh, UK,

⁵ School of Biological Sciences, University of Liverpool, Liverpool, UK and ⁶ Institute of Plant Biology, Biological Research Center, Szeged, Hungary

⁷ Present address: Division of Biology and Department of Applied Physics, California Institute of Technology, Pasadena, CA 91125, USA

* Corresponding authors. A Hall, School of Biological Sciences, University of Liverpool, Crown Street, Liverpool, UK. Tel.: +44 151 795 4565; Fax: +44 151 795 4403; E-mail: Anthony.hall@liverpool.ac.uk or A Millar, Institute of Molecular Plant Sciences, University of Edinburgh, Rutherford Building, Mayfield Road, Edinburgh EH9 3JH, UK. Tel.: +44 131 651 3325; Fax: +44 131 650 5392; E-mail: Andrew.Millar@ed.ac.uk

Received 26.7.06; accepted 14.8.06

Our computational model of the circadian clock comprised the feedback loop between *LATE ELONGATED HYPOCOTYL (LHY)*, *CIRCADIAN CLOCK ASSOCIATED 1 (CCA1)* and *TIMING OF CAB EXPRESSION 1 (TOC1)*, and a predicted, interlocking feedback loop involving *TOC1* and a hypothetical component *Y*. Experiments based on model predictions suggested *GIGANTEA (GI)* as a candidate for *Y*. We now extend the model to include a recently demonstrated feedback loop between the *TOC1* homologues *PSEUDO-RESPONSE REGULATOR 7 (PRR7)*, *PRR9* and *LHY* and *CCA1*. This three-loop network explains the rhythmic phenotype of *toc1* mutant alleles. Model predictions fit closely to new data on the *gi;lhy;cca1* mutant, which confirm that *GI* is a major contributor to *Y* function. Analysis of the three-loop network suggests that the plant clock consists of morning and evening oscillators, coupled intracellularly, which may be analogous to coupled, morning and evening clock cells in *Drosophila* and the mouse.

Molecular Systems Biology 14 November 2006; doi:10.1038/msb4100102

Subject Categories: metabolic and regulatory networks; plant biology

Keywords: circadian rhythm; genetic network; photoperiod; mathematical model; systems biology

Introduction

The circadian clock generates 24-h rhythms in most eukaryotes and in cyanobacteria (Dunlap *et al*, 2003), including the rhythmic expression of 5–15% of genes in eukaryotes (Duffield, 2003). Circadian rhythms are generated by a central network of 6–12 genes that form interlocked feedback loops (Glossop *et al*, 1999). The relatively small number of components involved in the circadian clock network makes it an ideal candidate for mathematical modelling of complex biological regulation (Ruoff and Rensing, 1996; Leloup and Goldbeter, 1998; Forger and Peskin, 2003).

The clock mechanism in the model plant, *Arabidopsis thaliana*, was first proposed to comprise a feedback loop in which two partially redundant genes, *LATE ELONGATED HYPOCOTYL (LHY)* and *CIRCADIAN CLOCK ASSOCIATED 1 (CCA1)*, repress the expression of their activator, *TIMING OF CAB EXPRESSION 1 (TOC1)* (Alabadi *et al*, 2001). This circuit cannot fit all experimental data (Locke *et al*, 2005a), as a short-period rhythm persists for several cycles both in *lhy;cca1* (Alabadi *et al*, 2002; Locke *et al*, 2005b) and in

toc1 mutant plants (Mas *et al*, 2003a). Previously we used mathematical modelling to propose a new circuit comprising two interlocking feedback loops in order to explain the residual rhythm in the *lhy;cca1* plant (Locke *et al*, 2005b). This model predicted the existence and expression patterns of two hypothetical components *X* and *Y*. *X* is proposed to be activated by *TOC1*, and *X* protein then activates *LHY* transcription, as required by the expression profile of *TOC1* protein (Mas *et al*, 2003b). *Y* forms a second loop with *TOC1*, which is responsible for the short-period oscillation in the *lhy;cca1* mutant. Based on the similarity of predicted and observed expression patterns, *GI* was identified as a candidate for *Y* (Locke *et al*, 2005b).

Here we have extended our model to include the recently proposed feedback loop between *PSEUDO-RESPONSE REGULATOR 7 (PRR7)*, *PRR9* and *LHY/CCA1* (Farre *et al*, 2005; Salome and McClung, 2005), resulting in a three-loop circuit (Figure 1A). We first validate this new model against existing and new experimental data. We then experimentally confirm our prediction that *GI* functions as a component of *Y* in a feedback loop with *TOC1*, and investigate the regulatory properties of the three-loop network.

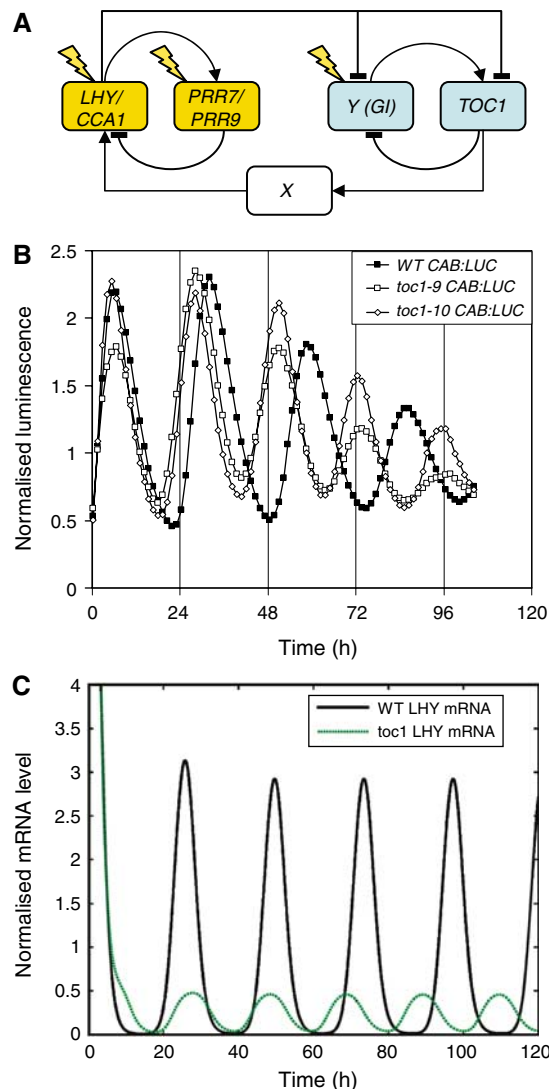


Figure 1 The three-loop *Arabidopsis* clock model accounts for 20 h rhythms in *toc1* mutants. **(A)** Summary of the three-loop network, showing only genes (boxed), regulatory interactions (arrows) and the locations of light input (flashes). Two-component oscillators are distinguished by shading the gene names in yellow or blue. **(B)** *CAB:LUCIFERASE (CAB:LUC)* rhythms in WT (filled squares), *toc1-9* (open squares) and *toc1-10* (open diamonds) under constant red light ($10 \mu\text{mol m}^{-2} \text{s}^{-1}$). Luminescence values were normalised to the average over the whole time course. Time zero is the onset of constant light (LL). **(C)** Simulated expression levels of *LHY* mRNA in the WT (black solid line) and *toc1* backgrounds (green dotted line) in LL. Expression levels were normalised to the average level of expression. Translation rate of *TOC1* mRNA in the simulated mutant is 1/1000 WT value.

Results

A three-loop clock network accounts for additional experimental data

A short-period rhythm can exist in mutants with reduced *TOC1* function in some conditions (Alabadi *et al*, 2001; Mas *et al*, 2003a). In order to test whether such residual rhythmicity was due to residual wild-type (WT) *TOC1* mRNA, we tested a *TOC1* deletion mutant (Supplementary information) for rhythmic expression of *CHLOROPHYLL A/B-BINDING PROTEIN2 (CAB2*,

also known as *LHCBI*1*), a morning-expressed clock output gene (Figure 1B). Plants of the *Ws* accession carrying the *toc1-10* deletion had a rhythm of 20 h period and reduced amplitude under constant light (LL) conditions. This was identical in timing to the rhythm of *toc1-9* plants, which carry a termination codon within the first domain of the predicted *TOC1* protein. Taken together, these data confirm previous suggestions that a *TOC1*-independent oscillator can persist in *toc1* plants (Mas *et al*, 2003a).

The proposed *PRR7/PRR9-LHY/CCA1* feedback loop provided a candidate mechanism to account for this oscillation. We therefore added this loop to the interlocked feedback model (Figure 1A; Supplementary information) to create a three-loop model. As the mutant phenotypes of *PRR7* and *9* are weak, apparently less than 1 h different from WT (Nakamichi *et al*, 2005), we grouped these genes together as one gene, *PRR7/9*, in our network equations (Supplementary information). *LHY* and *CCA1* were grouped together as *LHY* (Locke *et al*, 2005b). The first feedback loop involves *LHY* activating *PRR7/9* transcription (Farre *et al*, 2005), with *PRR7/9* protein going on to repress *LHY* activation. The remainder of the network follows our previous model (Locke *et al*, 2005b). *LHY* represses *TOC1* and *Y* transcription; the dual, repressing and activating role of *LHY* has experimental support (Harmer and Kay, 2005). *TOC1* protein activates *X* transcription, with *X* activating *LHY* transcription to form a second feedback loop. *Y* activates *TOC1* expression and *TOC1* represses *Y* expression, forming the third feedback loop. Light activates expression of *LHY*, *Y*, and now also *PRR7/9*, because *PRR9* has been shown to be acutely light-activated (Ito *et al*, 2003).

We used an extensive parameter search for the new and altered components to test whether the three-loop network could account for the residual oscillations of a *toc1* deletion mutant (Supplementary information). Our simulations show that the *PRR7/PRR9-LHY/CCA1* loop can generate the short-period rhythm of *toc1* plants (Figure 1C), and its absence can result in the very long period of *prp7;prp9* double mutants (Supplementary Figure 1; Farre *et al*, 2005). Neither of these observations could be accounted for with our interlocked feedback loop model (Locke *et al*, 2005b), which predicted arrhythmia or a long period under all conditions in simulations of a *toc1* null or loss-of-function mutants such as *toc1-2* (6% of WT RNA levels; Strayer *et al*, 2000) or the *toc1* RNAi lines (10–15%, Mas *et al*, 2003a). Sensitivity analysis shows that the three-loop model is similarly tolerant of parameter changes as the interlocking-loop model (Supplementary information; Supplementary Figure 2).

We now use the more realistic three-loop model to make further predictions for *Y*'s role in the clock, and test these predictions against the experimental manipulation of *GI*.

GI is a component of *Y*

A simulated *gi* mutation (modelled by reducing *Y* translation by 70%) gives a 1 h reduction in the period of *LHY* mRNA oscillations (Figure 2A), which matches well with the observed period of *CAB* expression rhythms in a *gi* null mutant background (Figure 2B). According to our models, the *Y-TOC1* feedback loop generates the 18 h rhythm seen in an *lhy;cca1* mutant (Figure 2C and D). A reduction in *Y* function in

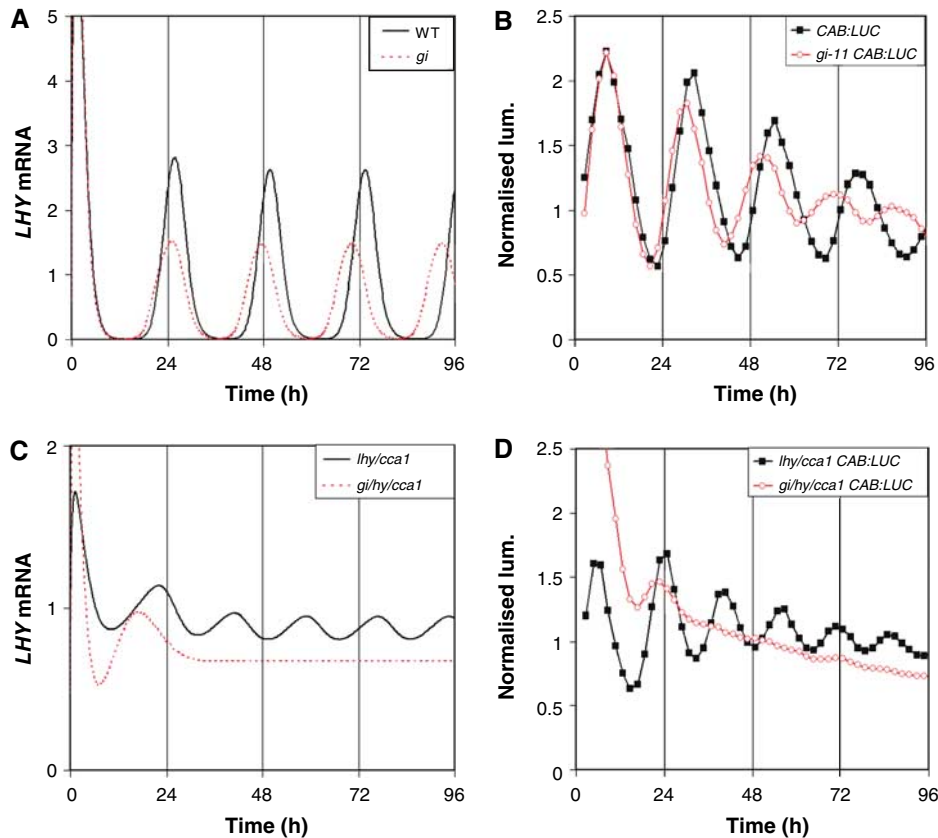


Figure 2 *GI* acts as *Y* in a feedback loop with *TOC1*. **(A)** Simulation of *LHY* mRNA levels in the WT (black solid line) and *gi* backgrounds (*Y* translation rate reduced by 70%, red dotted line) under constant light (LL). **(B)** Corresponding experimental data assaying circadian control of WT *CAB:LUC* expression by video imaging. **(C)** Simulation of *LHY* mRNA under LL in *lhy;cca1* (translation rate of *LHY* mRNA in simulated mutant is 1/1000 WT value, black line) and *gi;lhy;cca1* mutants (red dotted line). **(D)** Corresponding experimental data assaying *CAB:LUC* expression. The *gi;lhy;cca1* mutant is severely damped (only four out of 23 plants gave a period estimate within the circadian range, and those estimates had an average relative amplitude error of 0.86). All data were normalised to the average level of expression.

the *lhy;cca1* mutant background should therefore reduce the robustness of this residual rhythm. In fact, simulation of the *gi;lhy;cca1* triple mutation results in a rapid loss of rhythmicity, reaching a negligible amplitude during the second cycle in LL (Figure 2C). The very strong phenotype encouraged us to test the rhythms of *gi;lhy;cca1* triple mutant plants (Figure 2D). An almost exact match is made to the simulation; in the *gi;lhy;cca1* triple mutant, the rhythmic amplitude collapses to insignificance during the second cycle.

An identical, catastrophic damping is also seen experimentally in the rhythmic expression of *TOC1* and of *COLD AND CIRCADIAN REGULATED 2* (*CCR2*), an evening-expressed clock output gene, in the triple mutant under LL and constant darkness (DD) (Supplementary Figure 3), whereas the *lhy;cca1* double mutant retains short-period rhythms as described (Locke *et al*, 2005b). The mean level of *TOC1* expression is significantly reduced in the *gi;lhy;cca1* triple mutant compared with the *lhy;cca1* double mutant (Supplementary Figure 4A). This is consistent with *GI*'s functioning in the predicted role of *Y*, activating *TOC1*, and matches well to the expression levels in the simulated double and triple mutants (Supplementary Figure 4B). Our predictions also fit with experimental work showing that *GI* expression is light-responsive (Fowler *et al*, 1999; Paltiel *et al*, 2006), and are consistent with *GI* function in

balancing other clock components to generate temperature compensation (Gould *et al*, 2006). *GI* is a component of a light-activated feedback loop, separate from *LHY* and *CCA1*, which is required for the maintenance of residual rhythms in the *lhy;cca1* background.

Morning and evening oscillators allow tracking of dawn and dusk

Our three-loop model suggests a symmetrical structure for the *Arabidopsis* clock circuit. The model predicts that two short-period oscillators, the morning-expressed *PRR7/9-LHY/CCA1* loop and the evening-expressed *TOC1-Y/GI* loop, are coupled together by the *LHY/CCA1-TOC1-X* loop (Figure 1A). We investigated the effect of a change of photoperiod on the phase of the clock components of our three-loop network (Figure 3). The clock-regulated expression of *LHY* mRNA before dawn (20–24 h) remains at a fixed phase relative to dawn. In contrast, the peak of *TOC1* mRNA is delayed under long photoperiod conditions, showing that its phase also responds to the time of dusk. This flexibility is not seen in our one-loop or interlocked-loop models (Supplementary Figures 5 and 6), in which clock-regulated *LHY* and *TOC1* expressions are fixed

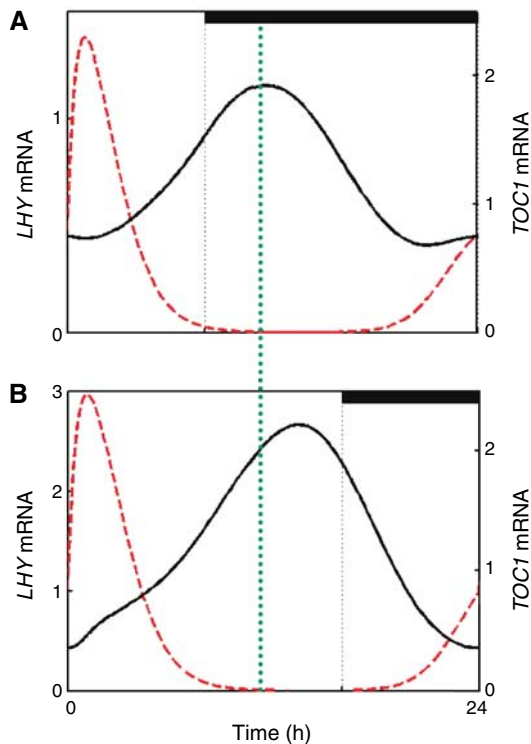


Figure 3 Three-loop network can track dawn and dusk. Simulations of *TOC1* mRNA (black solid line) and *LHY* mRNA (red dotted line) using the three-loop network under photoperiods of (A) LD8:16 and (B) LD16:8. The vertical dotted line highlights the shift in the peak phase of *TOC1* mRNA levels from LD8:16 to LD16:8. The peak phase of *LHY* mRNA is not shifted.

relative to dawn, or both move with the time of dusk. Note that *LHY* is light-induced in all the models, so its peak phase is forced by dawn. The three-loop structure of the clock provides the flexibility to track multiple phases (Rand *et al*, 2004).

The three-loop model also predicts that, if the coupling between *PRR7/9*–*LHY/CCA1* loop and the evening-expressed *TOC1*–*Y/GI* loop were impaired, the two oscillators might run with different periods within one cell. This is predicted by simulation of an *x* mutant (Supplementary Figure 7), where *LHY* mRNA levels oscillated with a 20.4 h period under LL conditions and *TOC1* levels oscillated with a 17.3 h period.

Discussion

We present evidence that *GI* acts with *TOC1* in a feedback loop of the circadian clock in *A. thaliana*. This marks an advance in systems biology, because *GI* was identified as a candidate gene in this loop using experiments based directly on predictions from mathematical modelling. The three-loop model has greater realism, as it can simulate the short-period rhythms of *toc1* and *gi* mutant plants and the long-period rhythms of *prp7;prp9* double mutants, while still correctly matching the mutant phenotypes accounted for by the previous model. Understanding the *Arabidopsis* clock as a system of coupled, morning and evening oscillators provides a new intellectual framework that may persist over multiple incremental advances in biochemical and genetic realism.

The three-loop model is not yet complete, as it does not incorporate known clock-affecting genes such as *PRR3*, *PRR5*, *TIME FOR COFFEE (TIC)*, *EARLY FLOWERING 4 (ELF4)* and *LUX ARRHYTHMO (LUX)* (reviewed by McClung, 2006). Rather than a weakness, this indicates three important uses of even incomplete mathematical models, in providing a framework to understand the existing experimental results, in focusing future experimental work on key regulatory interactions that reveal the location of the additional genes within the network and in informing the detailed design of these experiments, specifically to test any unusual aspect of regulation that has been predicted by simulation (Locke *et al*, 2005b).

The three-loop circuit contributes to the apparent robustness of the *Arabidopsis* clock, along with the partial redundancy of some genes: few single mutations alter the clock period by more than 3–4 h and arrhythmic mutations are rare (McClung, 2006). *GI*, one of the first characterised clock-affecting genes (Fowler *et al*, 1999; Park *et al*, 1999) with complex functions in both flowering and circadian regulation (Mizoguchi *et al*, 2005; Gould *et al*, 2006), illustrates the difficulty of understanding the effect of one component upon a complex network. The *gi* single mutant had a relatively weak phenotype, whereas our assays of the triple *gi;lhy;cca1* mutant demonstrate *GI*'s importance (Figure 2 and Supplementary Figure 3) as one component of *Y* in the three-loop network. It is likely that other components participate in the evening feedback loop with *TOC1*, because our current model indicates that the circadian phenotypes of the *gi* single mutant and the *gi;lhy;cca1* triple mutant are accurately simulated by a 70% reduction in *Y* translation, rather than a complete absence of *Y* (Figure 2 and Supplementary Figure 3). *PRR5* is a candidate component of *Y* that should now be tested, perhaps in combination with the *gi* mutation. If *PRR5* is indeed part of *Y*, then our model could explain the arrhythmicity of the *prp7;prp9;prp5* triple mutant (Nakamichi *et al*, 2005): the triple mutation not only removes the *PRR7/9* feedback loop, but also impairs the *TOC1*–*Y* feedback loop. Constructing such multiple mutants, in combination with reporter genes, is and will remain laborious. Insertional mutants in most *Arabidopsis* genes are publicly available, but there is no prospect of a comprehensive bank of double mutants. Modelling offers a crucial tool for targeting future mutant construction as well as for extracting the maximum value from time-series studies using existing genetic resources.

Analysis of the three-loop network suggests new avenues for experiments. For example, the prediction that an *x* mutation could lead to desynchronisation of two short-period clocks (Supplementary Figure 7) suggests that future research could target mutations or chemical manipulations that cause desynchronisation of *LHY* and *TOC1* mRNA rhythms. Period differences among rhythms in the same plant have been observed repeatedly and in some cases can be interpreted as evidence for desynchronisation of two intracellular oscillators, although cell-type-specific effects cannot be excluded (Hall *et al*, 2002; Michael *et al*, 2003). The three-loop model provides a mechanism for such intracellular desynchronisation, if the various rhythmic processes are controlled by different loops and coupling between loops is weakened in some conditions. This flexibility of circadian regulation is expected to offer a

selective advantage, particularly where seasonal changes in photoperiod vary the relative timing of dawn and dusk (Pittendrigh and Daan, 1976). There is strong evidence in *Drosophila* (Stoleru et al, 2004) and mammals (Jagota et al, 2000) for separate control of morning and evening processes by oscillators in different cells, which are coupled together by cell–cell signalling. Plant clocks are coupled only weakly between cells, if at all (Thain et al, 2000), but the three-loop circuit suggests that an analogous architecture can be constructed within a single cell, by coupling the loop of morning-expressed genes *LHY/CCA1* and *APPR7/9* to the evening-expressed *TOC1-GI* loop. It will now be important to understand the role and balance of the light inputs into each of the feedback loops of the clock, firstly to determine what flexibility the three-loop circuit could provide and then to understand how the plant has evolved to exploit this flexibility in controlling rhythmic functions at different times of day.

Note added in proof

Zeilinger et al, in a study published simultaneously in *Molecular Systems Biology*, add PRR7 and PRR9 in parallel feedback loops to the interlocked loop network, with an alternative parameter set and light input mechanisms to PRR9 and Y (Zeilinger et al, 2006).

Supplementary information

Supplementary information is available at the *Molecular Systems Biology* website (www.nature.com/msb).

Acknowledgements

We thank V Hibberd and A Thomson for technical assistance, and P Brown for constructing the SBML file of the three-loop model. JCWL was supported by a postgraduate studentship from the Gatsby Charitable Foundation. LKB was supported by a Marie Curie Fellowship. Computer facilities were provided by the Centre for Scientific Computing at the University of Warwick; low-light imaging facilities were supported in part by the University of Edinburgh. Research in Warwick and Edinburgh was funded by BBSRC grants G13967 and G19886 to AJM. Research at Liverpool was funded by BBSRC grant BBS/B/111125 and Royal Society grant R4917/1 award to AH. Research in Szeged was supported by a Howard Hughes Medical Institute International Scholarship to FN (grant no. HHMI 55005620). The authors declare that they have no competing financial interests.

References

Alabadi D, Oyama T, Yanovsky MJ, Harmon FG, Mas P, Kay SA (2001) Reciprocal regulation between *TOC1* and *LHY/CCA1* within the *Arabidopsis* circadian clock. *Science* **293**: 880–883

Alabadi D, Yanovsky MJ, Mas P, Harmer SL, Kay SA (2002) Critical role for *CCA1* and *LHY* in maintaining circadian rhythmicity in *Arabidopsis*. *Curr Biol* **12**: 757–761

Duffield GE (2003) DNA microarray analyses of circadian timing: the genomic basis of biological time. *J Neuroendocrinol* **15**: 991–1002

Dunlap JC, Loros JJ, De Coursey PJ (2003) *Chronobiology: biological timekeeping*. Sunderland, MA, USA: Sinauer Associates

Farre EM, Harmer SL, Harmon FG, Yanovsky MJ, Kay SA (2005) Overlapping and distinct roles of PRR7 and PRR9 in the *Arabidopsis* circadian clock. *Curr Biol* **15**: 47–54

Forger DB, Peskin CS (2003) A detailed predictive model of the mammalian circadian clock. *Proc Natl Acad Sci USA* **100**: 14806–14811

Fowler S, Lee K, Onouchi H, Samach A, Richardson K, Coupland G, Putterill J (1999) *GIGANTEA*: a circadian clock-controlled gene that regulates photoperiodic flowering in *Arabidopsis* and encodes a protein with several possible membrane-spanning domains. *EMBO J* **18**: 4679–4688

Glossop NRJ, Lyons LC, Hardin PE (1999) Interlocked feedback loops within the *Drosophila* circadian oscillator. *Science* **286**: 766–768

Gould PD, Locke JCW, Larue C, Southern MM, Davis SJ, Hanano S, Moyle R, Milich R, Putterill J, Millar AJ, Hall A (2006) The molecular basis of temperature compensation in the *Arabidopsis* circadian clock. *Plant Cell* **18**: 1177–1187

Hall A, Kozma-Bognar L, Bastow RM, Nagy F, Millar AJ (2002) Distinct regulation of *CAB* and *PHYB* gene expression by similar circadian clocks. *Plant J* **32**: 529–537

Harmer SL, Kay SA (2005) Positive and negative factors confer phase-specific circadian regulation of transcription in *Arabidopsis*. *Plant Cell* **17**: 1926–1940

Ito S, Matsushika A, Yamada H, Sato S, Kato T, Tabata S, Yamashino T, Mizuno T (2003) Characterization of the *APRR9* pseudo-response regulator belonging to the *APRR1/TOC1* quintet in *Arabidopsis thaliana*. *Plant Cell Physiol* **44**: 1237–1245

Jagota A, de la Iglesia HO, Schwartz WJ (2000) Morning and evening circadian oscillations in the suprachiasmatic nucleus *in vitro*. *Nat Neurosci* **3**: 372–376

Leloup JC, Goldbeter A (1998) A model for circadian rhythms in *Drosophila* incorporating the formation of a complex between the *PER* and *TIM* proteins. *J Biol Rhythms* **13**: 70–87

Locke JCW, Millar AJ, Turner MS (2005a) Modelling genetic networks with noisy and varied experimental data: the circadian clock in *Arabidopsis thaliana*. *J Theor Biol* **234**: 383–393

Locke JCW, Southern MM, Kozma-Bognar L, Hibberd V, Brown PE, Turner MS, Millar AJ (2005b) Extension of a genetic network model by iterative experimentation and mathematical analysis. *Mol Syst Biol* **1**: 13

Mas P, Alabadi D, Yanovsky MJ, Oyama T, Kay SA (2003a) Dual role of *TOC1* in the control of circadian and photomorphogenic responses in *Arabidopsis*. *Plant Cell* **15**: 223–236

Mas P, Kim WY, Somers DE, Kay SA (2003b) Targeted degradation of *TOC1* by *ZTL* modulates circadian function in *Arabidopsis thaliana*. *Nature* **426**: 567–570

McClung CR (2006) Plant circadian rhythms. *Plant Cell* **18**: 792–803

Michael TP, Salome PA, McClung CR (2003) Two *Arabidopsis* circadian oscillators can be distinguished by differential temperature sensitivity. *Proc Natl Acad Sci USA* **100**: 6878–6883

Mizoguchi T, Wright L, Fujiwara S, Cremer F, Lee K, Onouchi H, Mouradov A, Fowler S, Kamada H, Putterill J, Coupland G (2005) Distinct roles of *GIGANTEA* in promoting flowering and regulating circadian rhythms in *Arabidopsis*. *Plant Cell* **17**: 2255–2270

Nakamichi N, Kita M, Ito S, Yamashino T, Mizuno T (2005) PSEUDO-RESPONSE REGULATORS, PRR9, PRR7 and PRR5, together play essential roles close to the circadian clock of *Arabidopsis thaliana*. *Plant Cell Physiol* **46**: 686–698

Paltiel J, Amin R, Gover A, Ori N, Samach A (2006) Novel roles for *GIGANTEA* revealed under environmental conditions that modify its expression in *Arabidopsis* and *Medicago truncatula*. *Planta* advance online publication, 15 June 2006

Park DH, Somers DE, Kim YS, Choy YH, Lim HK, Soh MS, Kim HJ, Kay SA, Nam HG (1999) Control of circadian rhythms and photoperiodic flowering by the *Arabidopsis GIGANTEA* gene. *Science* **285**: 1579–1582

Pittendrigh CS, Daan S (1976) A functional analysis of circadian pacemakers in nocturnal rodents. V. A clock for all seasons. *J Comp Physiol A* **106**: 333–355

Rand DA, Shulgin BV, Salazar D, Millar AJ (2004) Design principles underlying circadian clocks. *J Roy Soc Interface* **1**: 119–130

- Ruoff P, Rensing L (1996) The temperature-compensated Goodwin model simulates many circadian clock properties. *J Theor Biol* **179**: 275–285
- Salome PA, McClung CR (2005) PSEUDO-RESPONSE REGULATOR 7 and 9 are partially redundant genes essential for the temperature responsiveness of the *Arabidopsis* circadian clock. *Plant Cell* **17**: 791–803
- Stoleru D, Peng Y, Agosto J, Rosbash M (2004) Coupled oscillators control morning and evening locomotor behaviour of *Drosophila*. *Nature* **431**: 862–868
- Strayer C, Oyama T, Schultz TF, Raman R, Somers DE, Mas P, Panda S, Kreps JA, Kay SA (2000) Cloning of the *Arabidopsis* clock gene TOC1, an autoregulatory response regulator homolog. *Science* **289**: 768–771
- Thain SC, Hall A, Millar AJ (2000) Functional independence of circadian clocks that regulate plant gene expression. *Curr Biol* **10**: 951–956
- Zeilinger MN, Farré EM, Taylor SR, Kay SA, Doyle III FJ (2006) A novel computational model of the circadian clock in *Arabidopsis* that incorporates PRR7 and PRR9. *Mol Syst Biol* **2**: 58

Supplemental methods

1 Experimental Methods

gi-11 was isolated in a screen of T-DNA insertion lines described in (Richardson *et al.*, 1998; Fowler *et al.*, 1999). The *CAB:LUC+* and *CCR2:LUC* transgenes in the WS background were as described in (Hall *et al.*, 2002) and (Doyle *et al.*, 2002), respectively. The *toc1-9* allele introduces a termination codon at W138 of TOC1, as described (Kevei *et al.*, 2006). *toc1-10* was isolated from a T-DNA mutagenised population (E.K., B.F. and F.N. unpublished data). The mutation is caused by a deletion that removes the coding region of TOC1 (At5g61380) after S255 and the adjacent gene (At5g61390, encoding an exonuclease-like protein). *toc1-9* and *toc1-10* were generated in the same WS *CAB:LUC* background (Hall *et al.*, 2002) and both alleles show indistinguishable photomorphogenic and circadian phenotypes. To create *TOC1:LUC*, a 2068 bp region upstream of the *TOC1* coding region was amplified (forward primer: tctagacttctctgaggaatttcac, reverse primer: ggatccgatcagattaacaactaac) and inserted into pZPΩLUC (Schultz *et al.*, 2001). The construct was transformed into wild type Ws plants. Transgenic lines carrying single insertion of the transgene were selected and characterised. The *cca1-11* and *lhy-21* mutants were isolated from the Arabidopsis Functional Genomics Consortium population (Krysan *et al.*, 1999) and these were used to produce a *lhy;cca1* double mutant. Both the double and single mutants have been described in (Hall *et al.*, 2003). The triple mutant was produced by crossing the *cca1-11;lhy-21* double mutant with *gi-11*. Late flowering plants were selected in the F2 generation and genotyped with 3 allele-specific mutant and WT primer sets. *CAB:LUC+* was transformed into both the *lhy;cca1* double and the *gi;lhy;cca1* triple mutants. At least 4 independently transformed lines expressing the luciferase construct were analysed for each genotype. The data in figure 2 is of one representative line. A *CCR2:LUC+* or *TOC1:LUC+* transgene was introgressed into both the *lhy;cca1* double and the *gi;lhy;cca1* triple mutants by genetic crossing.

2 Rhythm Analysis

The seedlings were then sown on Murashige-Skoog media contain 3% sucrose and 1.5% agar. Seeds were kept at 4°C for 2 days and then grown in 12L:12D cycles of 80 $\mu\text{mol m}^{-2}\text{s}^{-1}$ in a Sanyo MLR350 (Sanyo Gallenkamp PLC, UK). Temperatures both during entrainment and during experiments

were logged using Hobo temperature loggers (Onset computer corporation, USA). Luminescence levels were analysed using an ORCA-II-BT 1024, 16bit camera cooled to -80°C (Hamamatsu photonics, UK). The camera was housed on top of a Sanyo MIR-553 cooled incubator maintaining a uniform temperature $\pm 0.5^{\circ}\text{C}$ (Sanyo Gallenkamp PLC, UK). Illumination was provided by 4 red/blue LED arrays (MD electronics, UK). Image acquisition and light control was driven by WASABI imaging software (Hamamatsu photonics, UK). The images were processed using Metamorph 6.0 image analysis software (Molecular Devices corporation, USA). Alternatively, luminescence was recorded by an automated luminometer equipped by red and blue LED arrays, essentially as described (Hall *et al.*, 2002). Individual period estimates were generated by importing data into BRASS (available from www.amillar.org) and using BRASS to run fast fourier transform-nonlinear least squares (FFT NLLS) analysis programs (Plautz *et al.*, 1997) on each data trace to generate period estimates and relative amplitude errors (Rel. amp. Error). The data is representative of at least 2 independent experiments.

3 Computational Methods

We have built upon our network equations for the proposed interlocked feedback loop model for the Arabidopsis circadian clock (Locke *et al.*, 2005a), as a recent report suggests there is an additional feedback loop involving *LHY/CCA1* and the genes *PRR7* and *PRR9* (Farre *et al.*, 2005). The interlocked loop model consists of a feedback loop between *LHY*, which represents the function of both *CCA1* and *LHY* and is acutely light activated, and *TOC1*, and an additional loop between *TOC1* and a proposed gene *Y*, which is also light activated. An additional gene *X* is also proposed to be activated by *TOC1* and then go on to activate *LHY* transcription, as *TOC1* levels are low at dawn when *LHY* transcription is activated. We have added to this network an additional loop; *PRR7* and *PRR9* transcription is proposed to be activated by *LHY/CCA1*, and then *PRR7* and *PRR9* go on to repress *LHY* and *CCA1* transcription (Farre *et al.*, 2005). This gives us a three loop model for the clock (Figure 1).

We incorporated the *PRR7/9 - LHY/CCA1* feedback loop into the clock as follows. *PRR9* (Ito *et al.*, 2003) and *PRR7* (Yamamoto *et al.*, 2003) peak at the beginning and middle of the day respectively, with *PRR9* transcription acutely light activated. The functions of *PRR7* and *PRR9* in the clock are individually modest and hard to distinguish, notwithstanding their differing

light regulation, whereas the double *prp7;prp9* mutant gives a strong period phenotype (Farre *et al.*, 2005), so we combined their functions into a single gene in the model, termed *PRR7/9* (Eqns 14-16). *PRR7/9* transcription was given both an acute light activation term and a constant light activation term, as we previously used for *Y*, and is activated by nuclear LHY protein. However, our optimisation scheme minimised the parameters associated with the constant light activation of *PRR7/9*, so this term was removed from our equations for *PRR7/9* mRNA (Eqn 14).

We modified our terms for *LHY* mRNA levels to include the role of *PRR7/9* (Eqn 1). *PRR7/9* represses both *LHY*'s light activation and the activation by *TOC1*. In addition to the acute light reponse, we gave *LHY* mRNA levels a constant light activation term $\Theta_{\text{light}}(t)n_0$ as *LHY* transcription appears to be light activated throughout the day in an *prp7;prp9* plant (Farre *et al.*, 2005). $\Theta_{\text{light}} = 1$ when light is present, 0 otherwise.

We took the following as our mathematical model for the central circadian network, which involves the cellular concentrations $c_i^{(j)}(t)$ of the products of the i^{th} gene ($i = L$ labels LHY, $i = T$ labels TOC1, $i = X$ labels X, $i = Y$ label Y, $i = A$ labels *PRR7/9*) where $j = m, c, n$ denotes that it is the corresponding mRNA, or protein in the cytoplasm or nucleus respectively.

$$\frac{dc_L^{(m)}}{dt} = \left(\frac{g_0^\alpha}{(g_0^\alpha + c_A^{(n)\alpha})} \right) \left(\Theta_{\text{light}}(t) (q_1 c_P^{(n)} + n_0) + \frac{n_1 c_X^{(n)a}}{g_1^a + c_X^{(n)a}} \right) \times \frac{m_1 c_L^{(m)}}{k_1 + c_L^{(m)}} \quad (1)$$

$$\frac{dc_L^{(c)}}{dt} = p_1 c_L^{(m)} - r_1 c_L^{(c)} + r_2 c_L^{(n)} - \frac{m_2 c_L^{(c)}}{k_2 + c_L^{(c)}} \quad (2)$$

$$\frac{dc_L^{(n)}}{dt} = r_1 c_L^{(c)} - r_2 c_L^{(n)} - \frac{m_3 c_L^{(n)}}{k_3 + c_L^{(n)}} \quad (3)$$

$$\frac{dc_T^{(m)}}{dt} = \left(\frac{n_2 c_Y^{(n)b}}{g_2^b + c_Y^{(n)b}} \right) \left(\frac{g_3^c}{g_3^c + c_L^{(n)c}} \right) - \frac{m_4 c_T^{(m)}}{k_4 + c_T^{(m)}} \quad (4)$$

$$\frac{dc_T^{(c)}}{dt} = p_2 c_T^{(m)} - r_3 c_T^{(c)} + r_4 c_T^{(n)} - ((1 - \Theta_{\text{light}}(t))m_5 + m_6) \frac{c_T^{(c)}}{k_5 + c_T^{(c)}} \quad (5)$$

$$\frac{dc_T^{(n)}}{dt} = r_3 c_T^{(c)} - r_4 c_T^{(n)} - ((1 - \Theta_{\text{light}}(t))m_7 + m_8) \frac{c_T^{(n)}}{k_6 + c_T^{(n)}} \quad (6)$$

$$\frac{dc_X^{(m)}}{dt} = \frac{n_3 c_T^{(n)d}}{g_4^d + c_T^{(n)d}} - \frac{m_9 c_X^{(m)}}{k_7 + c_X^{(m)}} \quad (7)$$

$$\frac{dc_X^{(c)}}{dt} = p_3 c_X^{(m)} - r_5 c_X^{(c)} + r_6 c_X^{(n)} - \frac{m_{10} c_X^{(c)}}{k_8 + c_X^{(c)}} \quad (8)$$

$$\frac{dc_X^{(n)}}{dt} = r_5 c_X^{(c)} - r_6 c_X^{(n)} - \frac{m_{11} c_X^{(n)}}{k_9 + c_X^{(n)}} \quad (9)$$

$$\frac{dc_Y^{(m)}}{dt} = \left(\Theta_{\text{light}}(t) q_2 c_P^{(n)} + \frac{(\Theta_{\text{light}}(t) n_4 + n_5) g_5^e}{g_5^e + c_T^{(n)e}} \right) \times \left(\frac{g_6^f}{g_6^f + c_L^{(n)f}} \right) - \frac{m_{12} c_Y^{(m)}}{k_{10} + c_Y^{(m)}} \quad (10)$$

$$\frac{dc_Y^{(c)}}{dt} = p_4 c_Y^{(m)} - r_7 c_Y^{(c)} + r_8 c_Y^{(n)} - \frac{m_{13} c_Y^{(c)}}{k_{11} + c_Y^{(c)}} \quad (11)$$

$$\frac{dc_Y^{(n)}}{dt} = r_7 c_Y^{(c)} - r_8 c_Y^{(n)} - \frac{m_{14} c_Y^{(n)}}{k_{12} + c_Y^{(n)}} \quad (12)$$

$$\frac{dc_P^{(n)}}{dt} = (1 - \Theta_{\text{light}}(t)) p_5 - \frac{m_{15}c_P^{(n)}}{k_{13} + c_P^{(n)}} - q_3 \Theta_{\text{light}}(t) c_P^{(n)} \quad (13)$$

$$\frac{dc_A^{(m)}}{dt} = \Theta_{\text{light}}(t) \left(q_4 c_P^{(n)} \right) + \frac{n_6 c_L^{(n)g}}{g_7^g + c_L^{(n)g}} - \frac{m_{16}c_A^{(m)}}{k_{14} + c_A^{(m)}} \quad (14)$$

$$\frac{dc_A^{(c)}}{dt} = p_6 c_A^{(m)} - r_9 c_A^{(c)} + r_{10} c_A^{(n)} - \frac{m_{17}c_A^{(c)}}{k_{15} + c_A^{(c)}} \quad (15)$$

$$\frac{dc_A^{(n)}}{dt} = r_9 c_A^{(c)} - r_{10} c_A^{(n)} - \frac{m_{18}c_A^{(n)}}{k_{16} + c_A^{(n)}} \quad (16)$$

Here the various rate constants n_j , g_j etc parameterise transcription (n_j , g_j), degradation (m_j , k_j), translation (p_j), and the nuclear \leftrightarrow cytoplasmic protein transport (r_j). The Hill coefficients are represented by α , a , b , c , d , e , f , g . Light is known to give an acute, transient activation response for expression of *LHY* and *CCA1* (Kim *et al.*, 2003; Kaczorowski & Quail, 2003; Doyle *et al.*, 2002). This was modelled as in (Locke *et al.*, 2005a,b), using a simple mechanism involving an interaction of a light sensitive protein P, with concentration $c_P^{(n)}$ with the *LHY* gene promoter. $\Theta_{\text{light}} = 1$ when light is present, 0 otherwise. The values of the four parameters that appear in the equation for $c_P^{(n)}$ are chosen so as to give an acute light activation profile which is close to that observed in experiment. The essential features of Eq 13 are that P is produced only when light is absent and is degraded strongly when light is present.

3.1 Parameter Optimisation

The parameter values for the optimum solution for the interlocked feedback loop model (Locke *et al.*, 2005a) were taken as our starting point. In order to reduce parameter space, the acute light activation term for *PRR7/9* q_4 was set to the same value as the acute light response for the *LHY* promoter q_1 , g , the Hill coefficient of *PRR7/9* activation by *LHY* was set to the same value as c , the Hill coefficient of *TOC1* repression by *LHY*, and g_0 , the constant of repression of *LHY* by *APPR7/9* was set to 1. The value of the Hill coefficients were constrained through optimisation to take biological reasonable values of between 1 and 4, and the minimum value of the constant light activation term to *LHY*, n_0 , was set to 0.5, in order to ensure the possibility of light activation through out the day.

The parameters in Eqn 1 were reoptimised to take into account that in a *prr7;prr9* plant the period of the clock is approx 30 hours in LL (Farre

et al., 2005). In order to model the *prp7;prp9* mutation the translation rate of PRR7/9, p_6 , was set to 0, and then the equations were solved for 100000 simulated annealing points in order to minimise a qualitative cost function as defined in (Locke *et al.*, 2005a) which quantifies the goodness of fit of the solutions to several key pieces of experimental data. We briefly outline the terms of the cost function below, but for a full description of the method please see (Locke *et al.*, 2005a,b).

The equations were solved using MATLAB, integrated using the inbuilt stiff equation solver ODE15s (Shampine & Reichelt, 1997). The optimisation process described in the following sections was carried out by compiling the MATLAB code into C and running the code on a task farm super computer consisting of 31 x 2.6 GHz Pentium4 Xeon 2-way SMP nodes (62 CPUs in total). In order to evaluate the terms of the cost function, we solved numerically Eqns 1-16 over 600h, 300h in 12:12 LD cycles, and then 300h in LL conditions (the first 200h of each solution are discarded as transitory). In what follows we identify 1nM and 1h as the typical concentration and time scales, and measure all concentrations and rate constants in units where these are unity. We initialised our simulation at $c_i^{(j)} = 1$.

We made modifications to the WT cost function as defined for the interlocked loop model (Locke *et al.*, 2005a). We repeat a description of these terms here for completeness. The WT cost function is defined as:

$$\Delta = \delta_{\tau_{ld}} + \delta_{\tau_d} + \delta_{\phi} + \delta_{\text{size}} + \delta_{c_L} + \delta_{\phi_d} \quad (17)$$

we now describe each term of the cost function, Eqn.17, in turn.

First, $\delta_{\tau_{ld}}$ measures the difference between the experimental target period and the mean period of the oscillation in mRNA levels of *LHY* and *TOC1* in light:dark (LD) cycles as exhibited by the model;

$$\delta_{\tau_{ld}} = \sum_{i=L,T} \langle (24 - \tau_i^{(m)})^2 / 0.15 \rangle_{ld} \quad (18)$$

This is the summed error in the period, τ , for *LHY* (L) and *TOC1* (T) mRNA levels (m) in light:dark cycles (LD), where $\langle \rangle_{ld}$ gives the average over the cycles between $200 < t < 300$, and a marginally acceptable period difference of ≈ 25 mins contributes $O(1)$ to the cost function for each term.

Second, the term δ_{τ_d} gives a similar measure in constant darkness (DD). These two terms ensure that the entrained and free running clocks are near limit cycles with the experimentally observed period (stably entrained in LD cycles and with a free running period greater than 24h (Millar *et al.*, 1995)),

$$\delta_{\tau_d} = \sum_{i=L,T} \langle (25 - \tau_i^{(m)})^2 / f \rangle_d \quad (19)$$

where the average of $\langle \rangle_d$ is now over $300 < t < 600$ (DD). The biological evidence strongly indicates that the free running period of the clock is greater than 24 (Millar *et al.*, 1995), probably about 25, but we have less confidence in assigning a precise value hence we adopt values of $f = 0.05$ if $\tau_i^{(m)} \leq 25$ and $f = 2$ if $\tau_i^{(m)} > 25$.

Thirdly δ_ϕ measures the difference between the target phase and the average phase of the peaks of *LHY* and *TOC1* mRNA expression in LD. It also ensures that the oscillations are entrained to the LD cycles,

$$\delta_\phi = \sum_{i=L,T} \left[\langle \Delta\Phi_i^2 \rangle_{ld} + \left(\frac{\sigma[c_i^{(m)}(t_p)]_{ld}}{0.05 \langle c_i^{(m)}(t_p) \rangle_{ld}} \right)^2 + \left(\frac{\sigma[\Delta\Phi_i]}{5/60} \right)^2 \right] + \delta_{ent} \quad (20)$$

The first term compares the mean difference in phase over the LD cycles, where $\Delta\Phi_i = \bar{\phi}_i - \phi_i$, ϕ_i is the phase (from dawn) of the RNA peak in the model and $\bar{\phi}_L = 1hr$, $\bar{\phi}_T = 11hr$ are the target phases of the peaks in $c_L^{(m)}$ and $c_T^{(m)}$ respectively. We assume a cost that is $O(1)$ for solutions that differ by an hour. The next two terms ascribe a cost of $O(1)$ for limit cycle solutions in LD cycles whose peak heights vary only within 5 percent of one another, and whose variations in peak phases are 5 minutes. $\sigma[]_{ld}$ is the standard deviation for the cycles in LD. The term δ_{ent} checks that the solution is truly entrained to the light/dark cycle, i.e is not oscillating with the correct phase simply because of the initial conditions chosen. This is achieved as follows: the solution is rerun for 75h, taking the solution at 202h and shifting it back 3h, i.e initialising the $t = 202$ solution as the $t = 199$ solution. The new phase of the second peak is compared to the original phase of the second peak. If the phase discrepancy is still near 3 h, then the solution is too weakly entrained, and the solution is pathological. The LD cycles have failed to phase shift the response. We assume that the rate of adjustment of the phase is linear in the discrepancy of the phase. This gives us a phase discrepancy that goes to 0 exponentially in time (like the radioactive decay equation). The characteristic time is then trivially related to the log of the phase discrepancy. It is this logarithmic variation that is reflected in our choice of δ_{ent} . Hence δ_{ent} takes the form of $\log(0.5)/\log(\delta\phi/3)$, where $\delta\phi$ is the phase discrepancy in hours between the shifted and original solution, and $\delta\phi/3$ is therefore the fraction of the imposed 3h phase shift remaining after 2 periods. The term $\log(0.5)$ gives the acceptable remaining phase difference of 1.5h for the second cycle, which results in an $O(1)$ contribution to the cost function.

Next δ_{size} checks that the oscillation sizes are large enough to be detectable experimentally, and quantifies the degree to which the clock in the model is

damped in constant conditions: we require that it is not strongly damped,

$$\delta_{\text{size}} = \sum_{i=L,T} \left[\left(\frac{1}{\langle \Delta c_i^{(m)} \rangle_{ld}} \right)^2 + \left(\frac{\tau_o}{\tau_e} \right)^2 \right]. \quad (21)$$

The first term introduces a > 1 cost for solutions in LD cycle with oscillation sizes, $(\Delta c_i^{(m)} = c_{i \text{ max}}^{(m)} - c_{i \text{ min}}^{(m)})$, less than 1nm, and the second term penalises oscillations that decay too quickly when entering DD as follows: τ_o is a time characterising the decay in the oscillations over the 300h in DD, $\tau_o = -300/\log((\Delta c_T^{(m)}_{ld} - \Delta c_T^{(m)}_d)/\Delta c_T^{(m)}_{ld})$, and τ_e gives the marginally acceptable decay time, $-300/\log(0.75)$.

The term δ_{c_L} contains a measure of how broad the peak of *LHY* mRNA expression is in the proposed solution in LD cycles and is small only if the trace peaks sharply, as observed experimentally. This term is also only small if the peak heights of *LHY* mRNA expression drop when going from LD to DD,

$$\begin{aligned} \delta_{c_L} = & \sum_{i=2,-2} \left\langle \left(\frac{2/3c_L^{(m)}(t_p)}{c_L^{(m)}(t_p) - c_L^{(m)}(t_p + i)} \right)^2 \right\rangle_{ld} + \dots \\ & \left\langle \left(\frac{0.05(c_L^{(m)}(t_p - 2) - c_L^{(m)}(t_m))}{c_L^{(m)}(t_m) - c_L^{(m)}(t_m + i)} \right)^2 \right\rangle_{ld} + 10 \left(\frac{\langle c_L^{(m)}(t_p) \rangle_d}{\langle c_L^{(m)}(t_p) \rangle_{ld}} \right)^4 \end{aligned} \quad (22)$$

The first term penalises *LHY* mRNA expression profiles that do not have a sharp peak in LD cycles, with an $O(1)$ contribution if *LHY*'s expression level has dropped by 2/3 of its oscillation size within 2h before and after its peak of expression (at time t_p). The second term checks that *LHY* mRNA expression has a broad minimum, with an $O(1)$ contribution if 2h before and after the minimum point (at time t_m) *LHY*'s expression has only increased to 5 percent of the level 2 h before *LHY*'s peak. The last term checks that the peak of *LHY* mRNA expression drops from LD into DD, as it loses its acute light activation.

Finally, δ_{ϕ_d} constrains an appropriate phase difference between the peak times of *LHY* (ϕ_L) and *TOC1* mRNA (ϕ_T), $\Delta\Phi_d = \phi_T - \phi_L$ (modulo half the period), with a characteristic prefactor of 10h.

$$\delta_{\phi_d} = (10/\Delta\Phi_d)^2 \quad (23)$$

In order to model the *prr7;prr9* mutant the cost function error term for the WT period in DD, δ_{τ_d} was replaced with an error term for the period in LL,

$\delta_{\tau_{ll}}$ in order to find a solution in LL with a period of 30h, as opposed to a DD solution with a period of 25h. (Supplementary Table One, Supplementary figure 1).

$\delta_{\tau_{ll}}$ is given by:

$$\delta_{\tau_{ll}} = \sum_{i=L,T} \langle (30 - \tau_i^{(m)})^2 / f \rangle_{ll}. \quad (24)$$

This represents the summed error in the period, τ , for *LHY* (L) and *TOC1* (T) mRNA levels in constant light conditions, where $\langle \rangle_{ll}$ gives the average over the cycles between $300 < t < 600$. The biological evidence strongly indicates that the free running period of the clock in an *prr7;prr9* mutant plant is not less than 30h (Farre *et al.*, 2005), but we have less confidence in assigning a precise value hence we adopt values of $f = 0.05$ if $\tau_i^{(m)} \leq 30$ and $f = 2$ if $\tau_i^{(m)} > 30$. Also the error terms for the oscillation under constant conditions in δ_{size} and δ_{c_L} were calculated for LL, rather than DD.

The parameters for PPR7/9 were then optimised (Eqn 14-16) in order to model a WT plant. As in (Locke *et al.*, 2005a,b) the equations were solved for 1 million quasi random points in parameter space, and $\delta_{\tau_{ll}}$ was altered in order to search for a period in LL of 24h rather than 30h $\delta_{\tau_{ll}} = \sum_{i=L,T} \langle (24 - \tau_i^{(m)})^2 / 0.1 \rangle_{ll}$. The costfunction was also altered to find a short period oscillation in the *toc1* background (Mas *et al.*, 2003), as opposed to a short period oscillation in a *lhy;cca1* background (Locke *et al.*, 2005a). This gives a cost function:

$$\Delta = \delta_{\tau_{ld}} + \delta_{\tau_{ll}} + \delta_{\phi} + \delta_{size} + \delta_{c_L} + \delta_{\phi_d} + \delta_{\tau_{ld}}^{toc1} + \delta_{\tau_{ll}}^{toc1} + \delta_{\phi}^{toc1} + \delta_{size}^{toc1} + \delta_{c_Y}^{toc1} \quad (25)$$

where the first 6 WT terms are as defined as above, and the label (toc1) denotes the new cost function for the *toc1* mutant plant. We define below the terms for the new *toc1* mutant terms of the cost function:

$$\delta_{\tau_{ld}}^{toc1} = \sum_{i=A,L} \langle (24 - \tau_i^{(m)})^2 / 0.15 \rangle_{ld} \quad (26)$$

is the summed error in the period, τ , for *A* (PRR7/9) and *T* (*LHY*) mRNA (m) levels in LD cycles. We penalise solutions with a period of *PRR7/9* greater than 20 hours under constant light conditions. $\delta_{\tau_{ll}}^{(m)} = 0$ if the period is less than 20 hours, otherwise:

$$\delta_{\tau_{ll}}^{toc1} = \langle (20 - \tau_A^{(m)})^2 / 0.1 \rangle_{ll} \quad (27)$$

The next term δ_ϕ^{toc1} is defined as:

$$\delta_\phi^{toc1} = [\langle \Delta\Phi_L^2 \rangle_{ld} + (\sigma[\Delta\Phi_L])^2] \quad (28)$$

Here the first term compares the mean difference in phase over the LD cycles, where $\Delta\Phi_i = \bar{\phi}_L - \phi_L$, ϕ_L is the phase (from dawn) of the *LHY* mRNA peak in the model and $\bar{\phi}_L = 1h$ is the target phase of the peak in $c_L^{(m)}$. The second term describes a cost of $O(1)$ for solutions whose variations in peak phase are 1h. Next,

$$\delta_{size}^{toc1} = \sum_{i=A,L} \left(\frac{1}{\langle \Delta c_i^{(m)} \rangle_{ld}} \right)^2 \quad (29)$$

This term costs for solutions in LD cycle with oscillation sizes, $(\Delta c_i^{(m)} = c_{i_{max}}^{(m)} - c_{i_{min}}^{(m)})$, less than 1nm. Finally,

$$\delta_{c_Y}^{toc1} = \sum_{i=2,-2} \left\langle \left(\frac{2/3 c_L^{(m)}(t_p)}{c_L^{(m)}(t_p) - c_L^{(m)}(t_p + i)} \right)^2 \right\rangle_{ld} \quad (30)$$

The first term checks that the *LHY* mRNA expression profile has a sharp peak in LD cycles, with an $O(1)$ contribution if *LHY*'s expression level has dropped by 2/3 of its oscillation size within 2 hours before and after its peak of expression. As for previous optimisations, throughout the implementation the cost function was ‘‘capped’’ at $\Delta_{max} = 10^4$, such that $\Delta \rightarrow \text{Min}(10^4, \Delta)$. The sum of the *toc1* cost function terms was also capped at 10^3 .

The output of the model is the same as for the interlocked loop model when simulating a *lhy;cca1* plant, as PRR7/9 and LHY are no longer part of the functional clock in this case. A further 100000 simulated annealing points was carried out on the 10 best solutions found from the search of parameter space, to find the optimal parameter set (Supplementary Table One).

3.2 Parameter Stability Analysis

We examined the robustness of the optimised 3 loop model to parameter changes by calculating the period and amplitude of LHY mRNA oscillations over 300h in LL after a 5% increase or decrease of each parameter value in turn (Supplemental figure 2). The resulting change in period varied from 0 to 3%, similar to that seen for the interlocking loop model (Locke *et al.*, 2005a), and an improvement over the robustness properties for the one loop model (Locke *et al.*, 2005b). The model was most sensitive to alterations

in *PRR7/9* transcription and degradation (e.g see 4 points with mean *LHY* mRNA levels less than 0.5 in Supplemental figure 2). Longer transients after the transition from LD to LL are also seen using parameters with a 5% reduction in *PRR7/9* transcription compared to WT, although not in the transition from LD to DD (Data not shown). This further points to the need to investigate the role of light in the feedback loops.

References

- Doyle, M. R., Davis, Seth J., Bastow, R. M., McWatters, H. G., Kozma-Bognar, L., Nagy, F., Millar, A. J., & Amasino, R. 2002. The ELF4 gene controls circadian rhythms and flowering time in *Arabidopsis thaliana*. *Nature*, **132**, 732–238.
- Farre, E. M., Harmer, S. L., Harmon, F. G., Yanovsky, M. J., & Kay, S. A. 2005. Overlapping and distinct roles of PRR7 and PRR9 in the *Arabidopsis* circadian clock. *Curr. Biol.*, **15**(1), 47–54.
- Fowler, S., Lee, K., Onouchi, H., Samach, A., Richardson, K., Morris, B., Coupland, G., & Putterill, J. 1999. GIGANTEA: a circadian clock-controlled gene that regulates photoperiodic flowering in *Arabidopsis* and encodes a protein with several possible membrane-spanning domains. *EMBO J.*, **18**, 4679–4688.
- Hall, A., Kozma-Bognar, L., Bastow, R. M., Nagy, F., & Millar, A. J. 2002. Distinct regulation of CAB and PHYB gene expression by similar circadian clocks. *Plant J.*, **32**, 529–537.
- Hall, A., Bastow, R. M., Davis, S. J., Hanano, S., Mcwatters, H. G., Hibberd, V., Doyle, M. R., Sung, S., Amasino, K. J. Halliday R. M., & Millar, A. J. 2003. The TIME FOR COFFEE gene maintains the amplitude and timing of *Arabidopsis* circadian clocks. *Plant Cell*, **15**, 2719–2729.
- Ito, S., Matsushika, A., Yamada, H., Sato, S., Kato, T., Tabata, S., Yamashino, T., & Mizuno, T. 2003. Characterization of the APRR9 pseudo-response regulator belonging to the APRR1/TOC1 quintet in *Arabidopsis thaliana*. *Plant Cell Physiol.*, **44**, 1237–1245.
- Kaczorowski, K. A., & Quail, P. H. 2003. *Arabidopsis* PSEUDO-RESPONSE REGULATOR7 Is a Signaling Intermediate in Phytochrome-Regulated Seedling Deetiolation and Phasing of the Circadian Clock. *Plant Cell*, **15**, 2654–2665.

- Kevei, E., Gyula, P., Hall, A., Kozma-Bognar, L., W.Kim, Eriksson, M.E., Toth, R., Hanano, S., Feher, B., Southern, M.M., Bastow, R.M., Viczin, A., Hibberd, V., S.J.Davis, Somers, D.E., F.Nagy, & Millar, A.J. 2006. Forward genetic analysis of the circadian clock separates the multiple functions of ZEITLUPE. *Plant Physiol*, **140**, 944–945.
- Kim, J. Y., Song, H. R., Taylor, B. L., & Carre, I. A. 2003. Light-regulated translation mediates gated induction of the Arabidopsis clock protein LH1. *EMBO J.*, **22**, 935–944.
- Krysan, P. J., Young, J. C., & Sussman, M. R. 1999. T-DNA as an insertional mutagen in Arabidopsis. *Plant Cell*, **11**, 2283–2290.
- Locke, J C W, Southern, M M, Kozma-Bognar, L, Hibberd, V, Brown, P E, Turner, M S, & Millar, A J. 2005a. Extension of a genetic network model by iterative experimentation and mathematical analysis. *Mol Systems Biol*, **1**, 13.
- Locke, J. C. W., Millar, A. J., & Turner, M. S. 2005b. Modelling genetic networks with noisy and varied data: The circadian clock in *Arabidopsis Thaliana*. *J. Theor. Biology*, **234**, 383–393.
- Mas, P, Alabadi, D, Oyama, M J Yanovsky T, & Kay, S A. 2003. Dual Role of TOC1 in the control of circadian and photomorphogenic responses in Arabidopsis. *Plant Cell*, **15**, 223–236.
- Millar, A. J., Straume, M., Chory, J., Chua, N. H., & Kay, S. A. 1995. The regulation of circadian period by phototransduction pathways in Arabidopsis. *Science*, **267**, 1163–1166.
- Plautz, J. D., Straume, M., Stanewsky, R., Jamison, C. F., Brandes, C., Dowse, H. B., Hall, J. C., & Kay, S. A. 1997. Quantitative analysis of Drosophila period gene transcription in living animals. *J. Biol. Rhythms*, **12**(3), 204–217.
- Richardson, K., Fowler, S., Pullen, C., Skelton, C., Morris, B., & Putterill, J. 1998. T-DNA tagging of a flowering-time gene and improved gene transfer by in planta transformation of Arabidopsis. *Aust. J. Plant. Physiol.*, **25**(1), 125–130.
- Schultz, T.F., Kiyosue, T., Yanovsky, M., Wada, M., & Kay, S. A. 2001. A role for LKP2 in the circadian clock of Arabidopsis. *Plant Cell*, **13**, 2659–2670.

Shampine, L. F., & Reichelt, M. W. 1997. The MATLAB ODE Suite. *SIAM J. Sci. Comp.*, **18**, 1–22.

Yamamoto, Y., Sato, E., Shimizu, T., Nakamich, N., Sato, S., Kato, T., Tabata, S., Nagatani, A., Yamashino, T., & Mizuno, T. 2003. Comparative genetic studies on the APRR5 and APRR7 genes belonging to the APRR1/TOC1 quintet implicated in circadian rhythm, control of flowering time, and early photomorphogenesis. *Plant Cell Physiol.*, **44**, 1119–1130.

Supplemental Figure and Table Legends

Sup Figure 1) Simulation of *LHY* mRNA levels using the 3-loop model for WT and *prp7;prp9* mutant plants.

a) Comparison of simulated *LHY* mRNA levels in WT plant under constant light (LL) conditions (dotted line, left axis), with corresponding experimental data extracted from (Farre et al., 2005) (solid line, right axis).

b) Comparison of simulated *LHY* mRNA levels in *prp7;prp9* plant under constant LL conditions (dotted line, left axis), with corresponding experimental data extracted from (Farre et al., 2005) (solid line, right axis). Translation rate of *PRP7/9* mRNA in simulated mutant is 1/1000 WT value.

Sup Figure 2) Stability analysis of optimal parameter set in the 3-loop model.

The period and amplitude of *LHY* mRNA oscillations over 300h in LL are calculated for a 5% increase and decrease to each parameter in turn. The red circle represents the period and amplitude of the simulation using the optimal parameter values.

Sup Figure 3) Comparison of 3-loop model simulations of *TOC1* mRNA levels for WT, *lhy;cca1*, and *gi;lhy;cca1* plants to data.

a) Simulation of *TOC1* mRNA levels in WT (Black line), *lhy;cca1* (green line) and *gi;lhy;cca1* (red line) in LL conditions.

b) Simulation of *TOC1* mRNA levels in WT (Black line), *lhy;cca1* (green line) and *gi;lhy;cca1* (red line) in DD conditions.

c-f) Experimental data showing *TOC1:LUC* (C,E) and *CCR2:LUC* (D,F) expression patterns in WT (solid black line) *lhy;cca1* double (solid green line) and *gi;lhy;cca1* triple (solid red line) mutants under constant red/blue light (c,d) or constant dark (E,F) conditions. Luminescence values were normalised to the average of counts recorded during the course of the experiment. Time zero corresponds to the onset of the constant conditions (c,d) or to the time of the first subjective dawn (e,f). White and black bars indicate constant light or dark conditions, respectively.

Sup Figure 4) Simulations and experimental data for mean *TOC1* mRNA levels in WT, *lhy;cca1* and *gi;lhy;cca1* mutant plants.

a) Experimental data showing mean expression levels of *TOC1:LUC* in WT, *lhy;cca1* double and *gi;lhy;cca1* triple mutant under constant red/blue light (white bars) or constant dark (black bars). Luminescence counts were recorded at 1-2 hr intervals for five days under the specified light condition. Error bars represent standard error values.

b) Simulated mean expression levels of *TOC1* for WT, *lhy;cca1*, and *gi;lhy;cca1* conditions in LL (white bars) and DD (black bars).

Sup Figure 5) Simulations of effect of change in photoperiod on *TOC1* and *LHY* mRNA levels for one loop LHY/CCA1 – TOC1 network (Locke et al., 2005a). a) *LHY* mRNA levels and b) *TOC1* mRNA levels under LD8:16. c) *LHY* and d) *TOC1* mRNA levels under LD16:8 conditions.

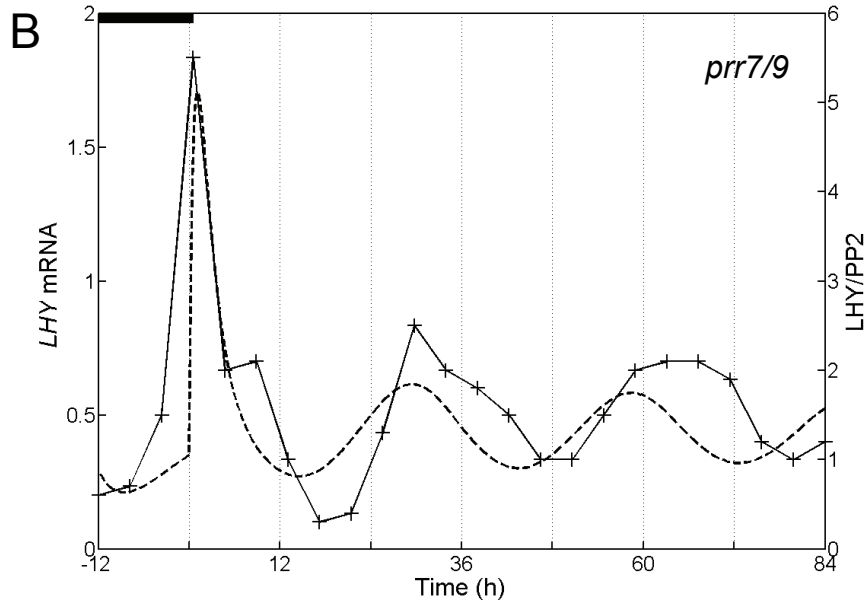
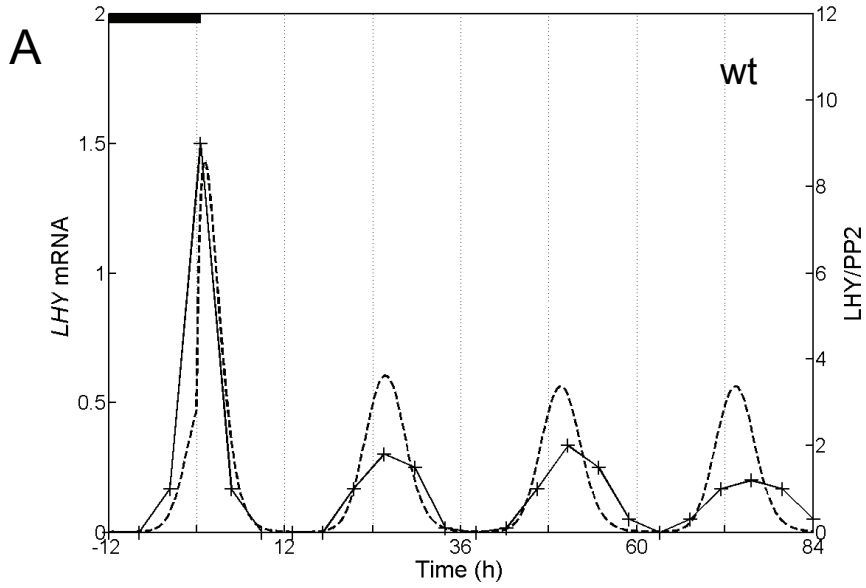
Sup Figure 6) Simulations of effect of change in photoperiods on *TOC1* and *LHY* mRNA levels for interlocked feedback loop network (Locke et al., 2005b). a) *LHY* mRNA levels and b) *TOC1* mRNA levels under LD8:16. c) *LHY* and d) *TOC1* mRNA levels under LD16:8.

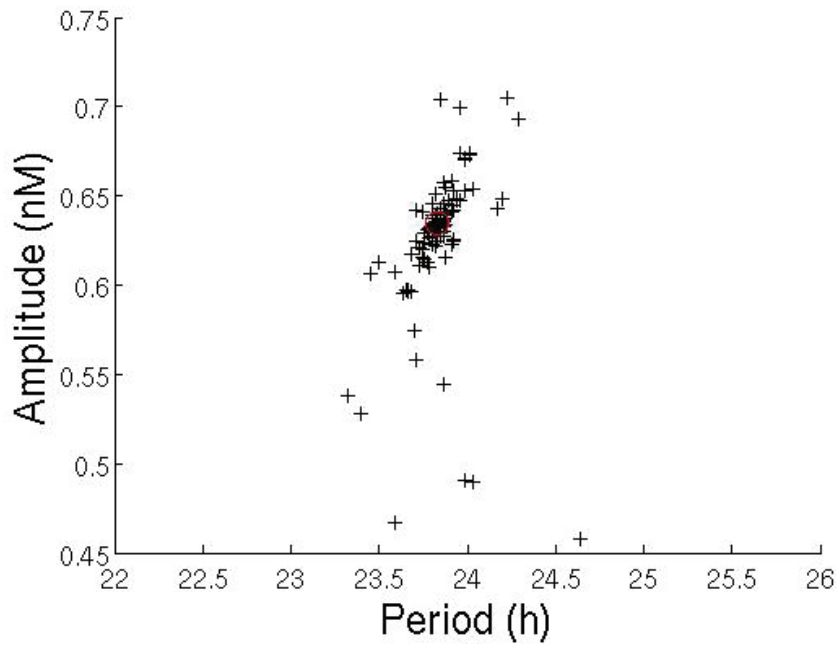
Sup Figure 7) An *x* mutation can de-couple the two clocks. Simulation of *LHY* mRNA levels and *TOC1* mRNA levels in an *x* mutant background, shown for an interval of free running rhythm in LL. Translation rate of *X* mRNA in simulated mutant is 1/1000 WT value. Peak levels of *TOC1* and *LHY* mRNA can be seen to go in and out of phase with each other. Data was normalised to the maximum level of expression.

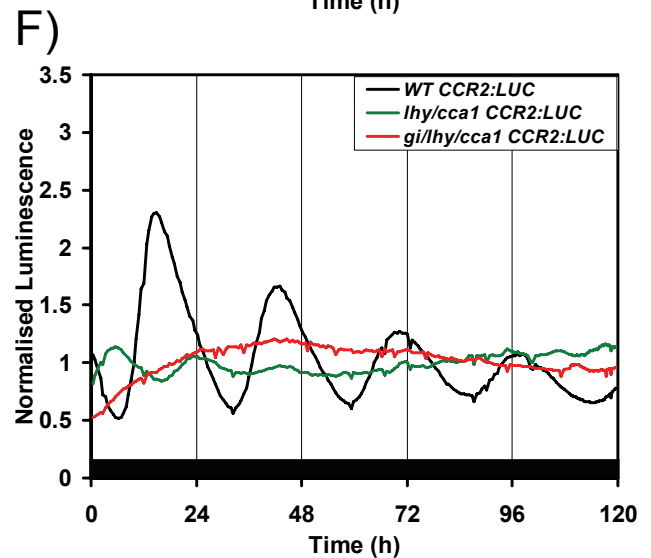
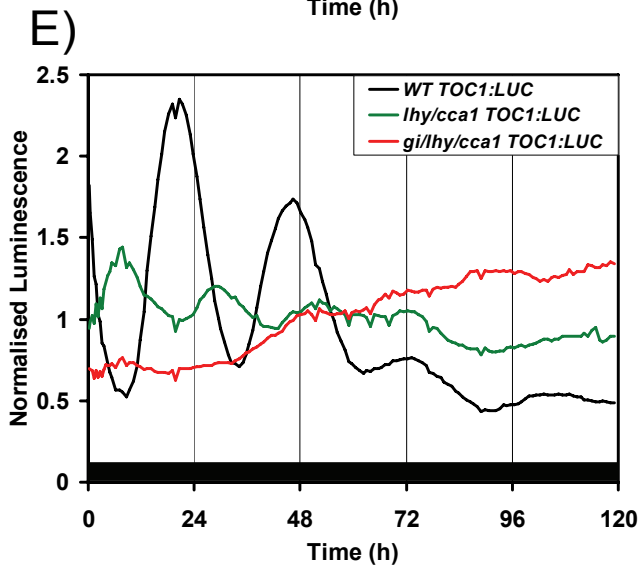
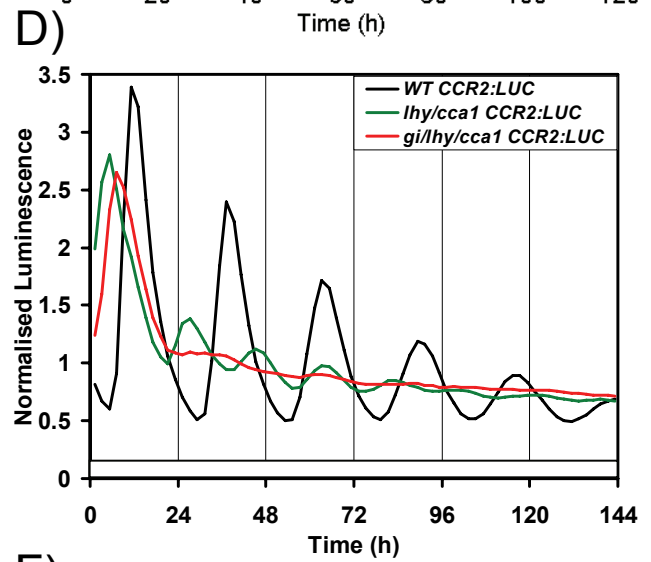
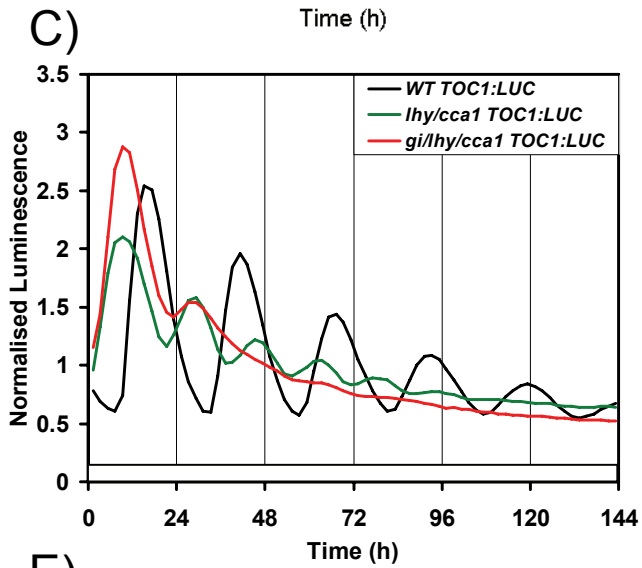
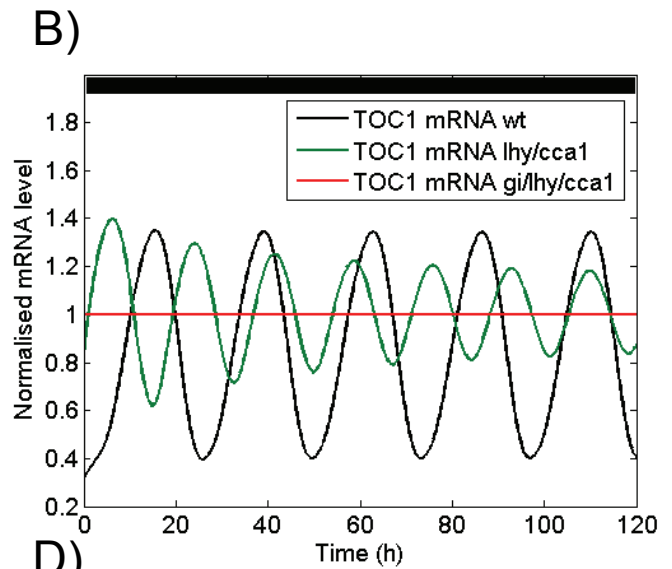
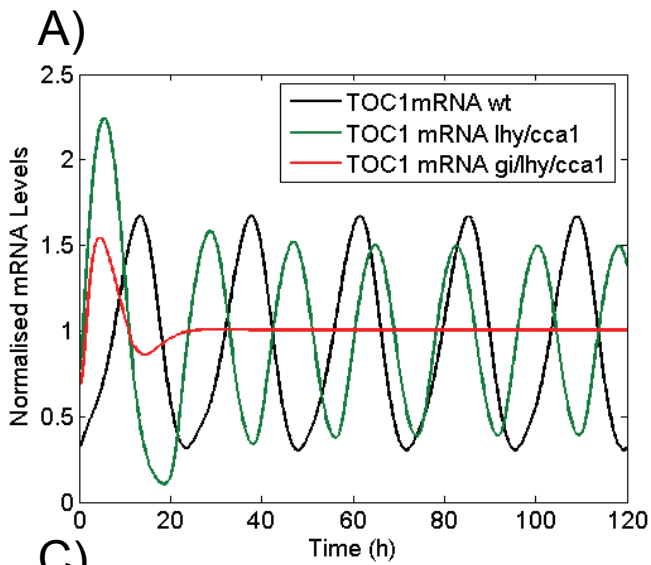
Sup Table 1) Optimal parameter values for the 3-loop model.

References

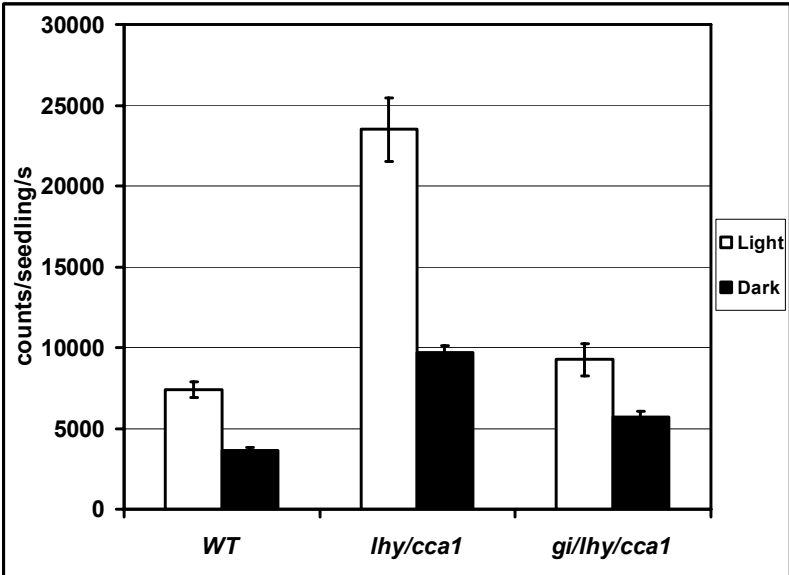
- Farre, E.M., Harmer, S.L., Harmon, F.G., Yanovsky, M.J. and Kay, S.A. (2005) Overlapping and distinct roles of PRR7 and PRR9 in the Arabidopsis circadian clock. *Curr Biol*, **15**: 47-54
- Locke, J.C., Millar, A.J. and Turner, M.S. (2005a) Modelling genetic networks with noisy and varied experimental data: the circadian clock in *Arabidopsis thaliana*. *J Theor Biol*, **234**: 383-393
- Locke, J.C.W., Southern, M.M., Kozma-Bognar, L., Hibberd, V., Brown, P.E., Turner, M.S. and Millar, A.J. (2005b) Extension of a genetic network model by iterative experimentation and mathematical analysis. *Mol Syst Biol*, **1**: 13, doi:10.1038/msb4100018



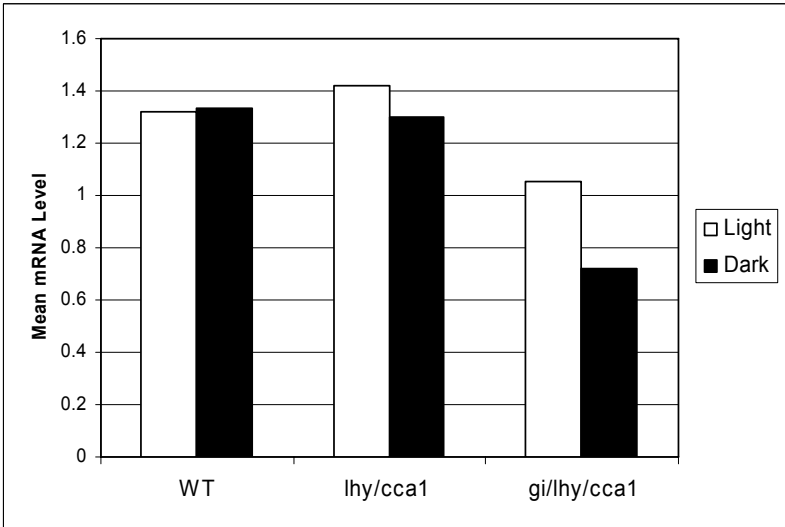


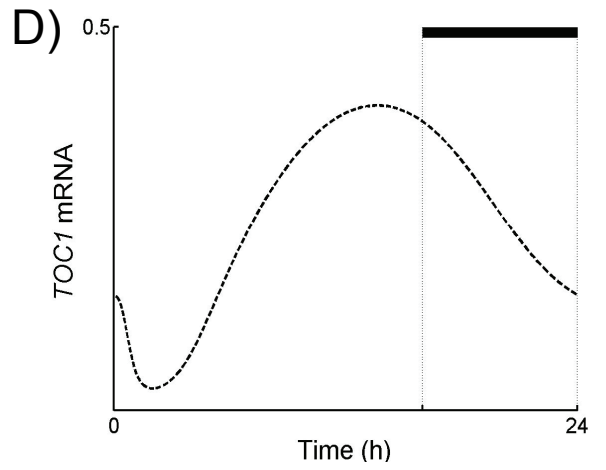
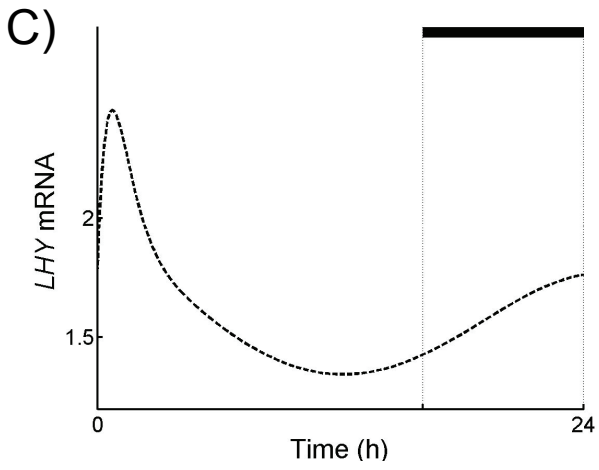
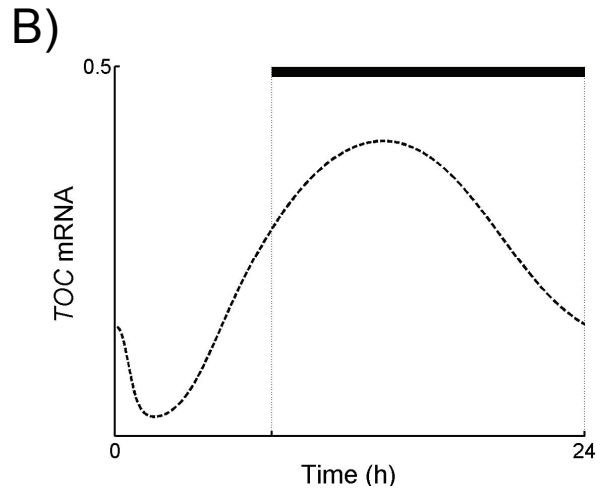
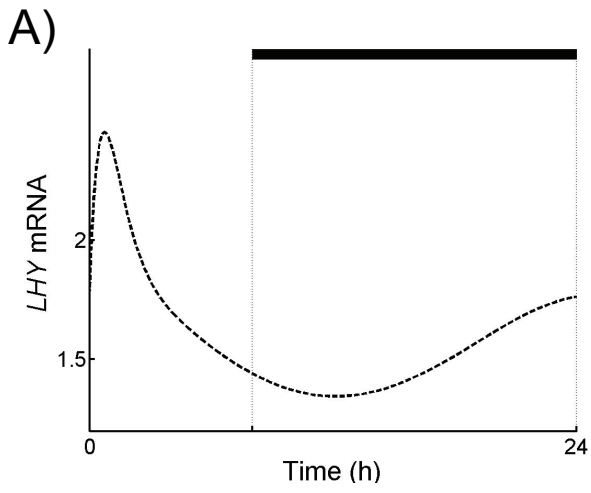


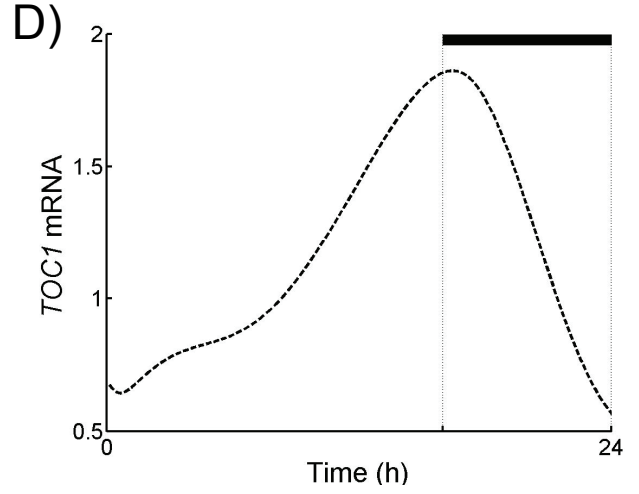
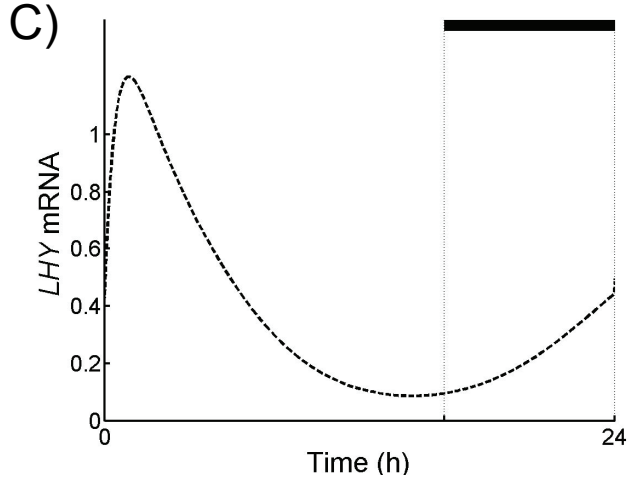
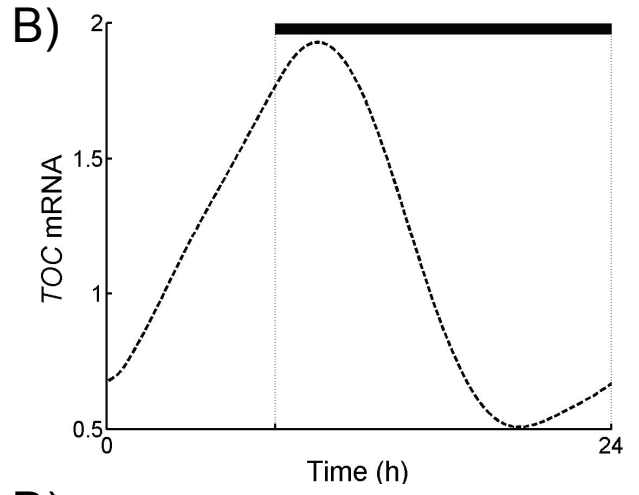
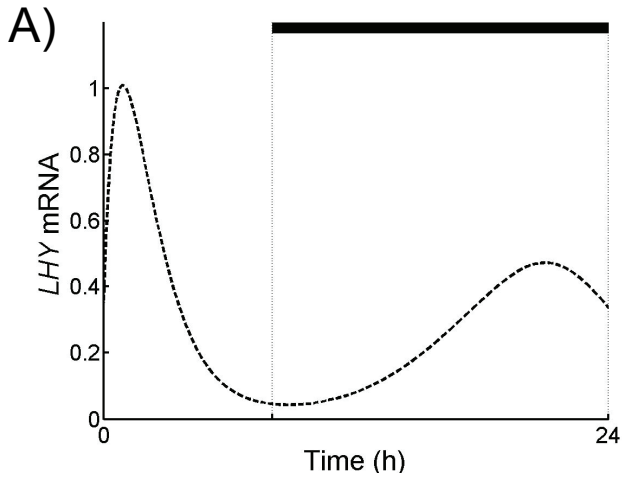
A)

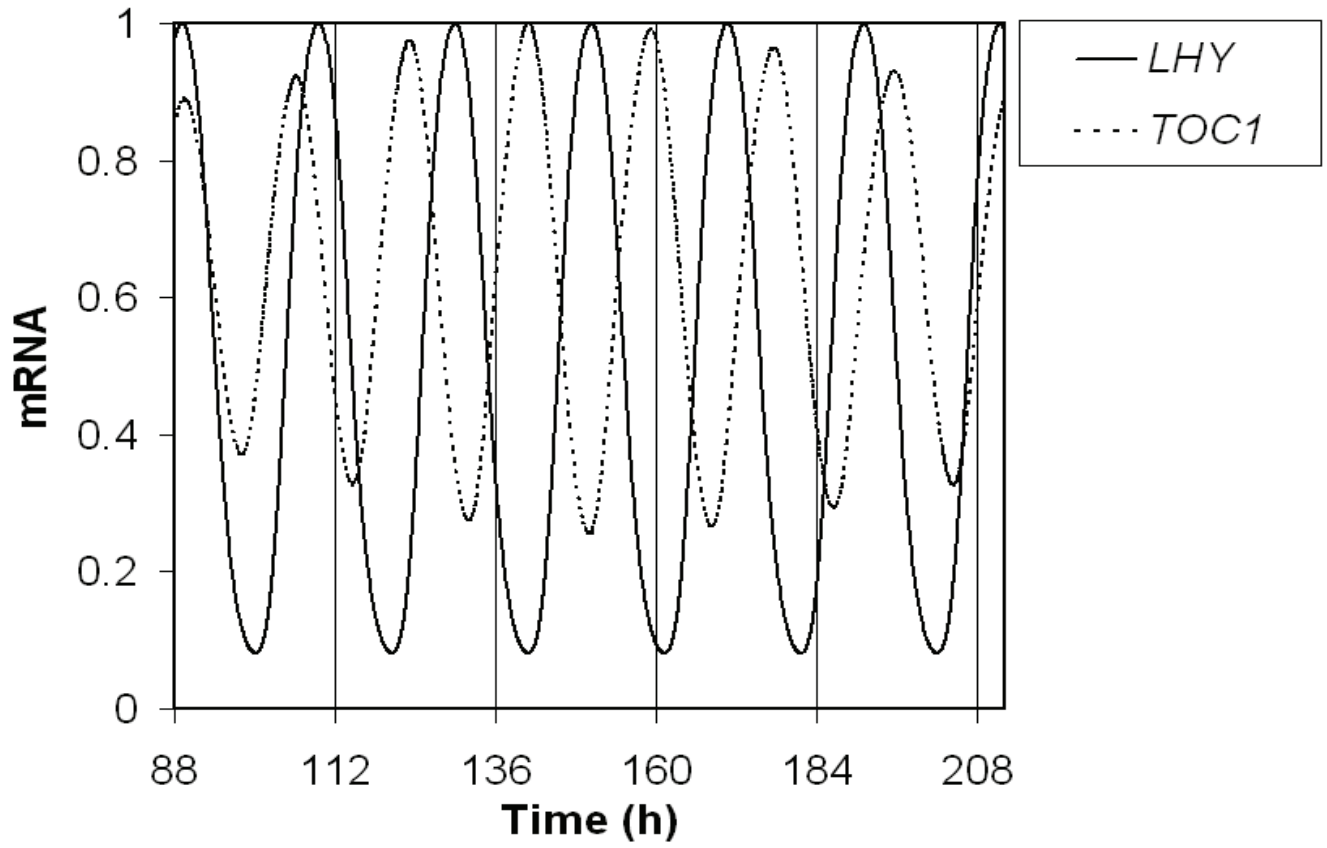


B)









Parameter values for 3 – loop model of Arabidopsis clock			
Parameter Name	Parameter Value	Parameter Description	Dimensions
q1	4.1954	Coupling constant of light activation of LHY transcription	1/h
n0	0.0500	Maximum light-dependent LHY transcription rate	nM/h
g0	1	Maximum light-dependent LHY transcription rate	nM/h
α	4.000	Constant of repression by APPR7/9	nM
n1	7.8142	Maximum light-independent LHY transcription rate	nM/h
a	1.2479	Hill coefficient of activation by protein X	
g1	3.1383	Constant of activation by protein X	nM
m1	1.9990	Maximum rate of LHY mRNA degradation	nM/h
k1	2.3920	Michaelis constant of LHY mRNA degradation	nM
p1	0.8295	Rate constant of LHY mRNA translation	1/h
r1	16.8363	Rate constant of LHY transport into nucleus	1/h
r2	0.1687	Rate constant of LHY transport out of nucleus	1/h
m2	20.4400	Maximum rate of cytoplasmic LHY degradation	nM/h
k2	1.5644	Michaelis constant of cytoplasmic LHY degradation	nM
m3	3.6888	Maximum rate of nuclear LHY degradation	nM/h
k3	1.2765	Michaelis constant of nuclear LHY degradation	nM
n2	3.0087	Maximum TOC1 transcription rate	nM/h
b	1.0258	Hill coefficient of activation by protein Y	
g2	0.0368	Constant of activation by protein Y	nM
g3	0.2658	Constant of repression by LHY	nM
c	1.0258	Hill coefficient of repression by LHY	
m4	3.8231	Maximum rate of TOC mRNA degradation	nM/h
k4	2.5734	Michaelis constant of TOC mRNA degradation	nM
p2	4.3240	Rate constant of TOC1 mRNA translation	1/h
r3	0.3166	Rate constant of TOC1 movement into nucleus	1/h
r4	2.1509	Rate constant of TOC1 movement out of nucleus	1/h
m5	0.0013	Maximum rate of light dependent cytoplasmic TOC1 degradation	nM/h
m6	3.1741	Maximum rate of light independent cytoplasmic TOC1 degradation	nM/h
k5	2.7454	Michaelis constant of cytoplasmic TOC1 degradation	nM
m7	0.0492	Maximum rate of light dependent nuclear TOC1 degradation	nM/h
m8	4.0424	Maximum rate of light independent nuclear TOC1 degradation	nM/h

Parameter Name	Parameter Value	Parameter Description	Dimensions
k6	0.4033	Michaelis constant of nuclear TOC1 degradation	nM
n3	0.2431	Maximum transcription rate of protein X	nM/h
d	1.4422	Hill coefficient of activation by TOC1	
g4	0.5388	Constant of activation by TOC1	nM
m9	10.1132	Maximum rate of degradation of protein X mRNA	nM/h
k7	6.5585	Michaelis constant of protein X mRNA degradation	nM
p3	2.1470	Rate constant of X mRNA translation	1/h
r5	1.0352	Rate constant of protein X movement into nucleus	1/h
r6	3.3017	Rate constant of protein X movement out of nucleus	1/h
m10	0.2179	Maximum rate of degradation of cytoplasmic protein X	nM/h
k8	0.6632	Michaelis constant of cytoplasmic protein X degradation	nM
m11	3.3442	Maximum rate of degradation of nuclear protein X	nM/h
k9	17.1111	Michaelis constant of nuclear protein X degradation	nM
q2	2.4017	Coupling constant of light activation of Y mRNA transcription	1/h
n4	0.0857	Light dependent component of Y transcription	nM/h
n5	0.1649	Light independent component of Y transcription	nM/h
g5	1.1780	Constant of repression by TOC1	nM
g6	0.0645	Constant of repression by LHY	nM
e	3.6064	Hill coefficient of repression by TOC1	
f	1.0237	Hill coefficient of repression by LHY	
m12	4.2970	Maximum rate of degradation of protein Y mRNA	nM/h
k10	1.7303	Michaelis constant of protein Y mRNA degradation	nM
p4	0.2485	Rate constant of Y mRNA translation	1/h
r7	2.2123	Rate constant of protein Y movement into nucleus	1/h
r8	0.2002	Rate constant of protein Y movement out of nucleus	1/h
m13	0.1347	Maximum rate of degradation of cytoplasmic protein Y	nM/h
k11	1.8258	Michaelis constant of cytoplasmic protein Y degradation	nM
m14	0.6114	Maximum rate of degradation of nuclear protein Y	nM/h
k12	1.8066	Michaelis constant of nuclear protein Y degradation	nM
p5	0.5000	Light dependent production of protein P	nM/h
k13	1.2000	Michaelis constant of protein P degradation	nM
m15	1.2000	Maximum rate of protein P degradation	nM/h
q3	1.0000	Coupling constant of light activation of protein P degradation	1/h

Parameter Name	Parameter Value	Parameter Description	Dimensions
q4	2.4514	Coupling constant of light activation of LHY transcription	1/h
g	1.0258	Hill coefficient of activation by LHY	
n6	8.0706	Maximum light-independent APRR7/9 transcription rate	nM/h
n7	0.0002	Maximum light-dependent APRR7/9 transcription rate	(nM/h)(nM) ^g
g7	0.0004	Constant of activation by LHY	nM
m16	12.2398	Maximum rate of degradation of APRR7/9 mRNA	nM/h
k14	10.3617	Michaelis constant of APRR7/9 mRNA degradation	nM
p6	0.2907	Rate constant of APRR7/9 mRNA translation	1/h
r9	0.2528	Rate constant of APRR7/9 protein movement out of nucleus	1/h
r10	0.2212	Rate constant of APRR7/9 protein movement into the nucleus	1/h
m17	4.4505	Maximum rate of degradation of cytoplasmic protein APRR7/9	nM/h
k15	0.0703	Michaelis constant of cytoplasmic protein APRR7/9 degradation	nM
m18	0.0156	Maximum rate of degradation of nuclear protein APRR7/9	nM/h
k16	0.6104	Michaelis constant of nuclear protein APRR7/9 degradation	nM